

Equilibration dynamics of a dynamic covalent network diluted in a metallo-supramolecular polymer matrix

Rowanne Lyons¹, Larissa Hammer², Alexis André¹, Charles-André Fustin^{1*}, Renaud
Nicolaÿ², Evelyne van Ruymbeke^{1*}

1. *Institute of Condensed Matter and Nanosciences (IMCN), Bio- and Soft Matter division (BSMA), Université catholique de Louvain, Place Pasteur 1 and Place Croix du Sud 1, Louvain-la-Neuve B-1348, Belgium*

2. *Chimie Moléculaire, Macromoléculaire, Matériaux, ESPCI Paris, Université PSL, CNRS, 75005 Paris, France.*

*: charles-andre.fustin@uclouvain.be; Evelyne.vanruymbeke@uclouvain.be

ABSTRACT:

We investigate the viscoelastic properties of double dynamic networks based on side-functionalized PnBA chains. One of these networks is highly crosslinked by metal-ligand junctions characterized by a fast association/dissociation dynamics, while the other network is sparsely crosslinked with slow dynamic covalent bonds (DCN). We first show that modulating the dynamics of the metallo-supramolecular networks, by playing with the temperature, the density of reversible junctions or the stress applied, has direct consequences on the local equilibration of the DCN. The latter takes place by a Constraint Release Rouse process, at the rhythm of the association/dissociation of the metal-ligand junctions. Then, based on creep-recovery experiments, we investigate the ability of the double dynamic networks to recover their initial shape after a creep test, and show again the important role played by the metallo-supramolecular network. In particular, the sample recovery strongly depends on the network connectivity, which is enhanced if a denser metallo-supramolecular network is used, as it reduces the possible creep of the double dynamic network and increases its elastic memory. The sample recovery also depends on the association-dissociation dynamics of the metallo-supramolecular bonds, as it fixes how fast the stretched DCN can come back to its equilibrium conformation and can recover its initial shape after a large deformation has been applied. Adjusting the dynamics of the weak network is thus a key process to govern the viscoelastic response of the slow network.

This is the author's peer reviewed, accepted manuscript. However, the online version of record will be different from this version once it has been copyedited and typeset.
PLEASE CITE THIS ARTICLE AS DOI: 10.1122/1.5000047

I. Introduction

Supramolecular polymer chemistry is a rich and varied field involving non-covalent interactions between molecular or macromolecular units. These interactions range from van der Waals forces to hydrogen bonds to metal-ligand bonds, and can be used to build a variety of polymeric materials such as linear, branched and star-like polymers, or polymer networks. Polymer networks crosslinked via supramolecular interactions are more customizable in bond strength and dynamics than networks based on static covalent bonds, which allow preparing materials presenting a wide range of mechanical properties. Due to these characteristics, networks based on supramolecular bonds show high capacity for self-healing, toughness and elasticity.¹⁻⁶

Designing polymer networks is a trade-off between the mechanical strength, resistance to creep, extensibility and breakage resistance.⁷⁻⁹ Usually, improving one of these properties will negatively affect at least one of the other ones. In order to overcome this limitation, double networks were first created by Gong et al¹⁰ to make an exceptionally tough hydrogel. Using two interpenetrating polymer networks, the system captures the advantages of each sub-networks while eliminating their disadvantages. More specifically, a highly crosslinked network was first formed in aqueous solution, which was subsequently interpenetrated by a second loosely crosslinked network. These double network hydrogels were proven to withstand higher compression and have more resistance to fracture, as compared to the individual networks. In the years since, double networks have become more popular, both as gels and elastomers.¹¹⁻²² A synergistic effect exists between the two sub-networks, leading to an increased viscoelastic modulus,²⁰ increased adhesion,²¹ or increased compressive strength,²² to provide a few examples.

Among double networks, double dynamic networks (DDN), i.e., networks containing two distinct types of crosslinks exhibiting different dynamics, such as supramolecular and covalent bonds, allow to increase the material toughness while providing more control over the material properties, as compared to systems based on a single type of crosslinks. Indeed, tensile testing on such systems have shown the beneficial effect of the more dynamic network on the sample extensibility and self-healing ability. For example, Jiang et al¹⁵ showed that a dynamic network based on metal-ligand interactions and interpenetrated with a chemically crosslinked network is more ductile and resistant to fracture compared to the network without metal ions added. Moreover, cyclic tensile testing confirmed the ability of this sample to recover its initial shape, which requires however that the dissociation and reformation of the non-covalent links have time to take place. More precisely, with such materials, significant hysteresis is usually observed in the first loading–unloading cycle, due to the energy dissipation induced by the rupture of the reversible junctions.²³⁻²⁵ If the second cycle is applied

This is the author's peer reviewed, accepted manuscript. However, the online version of record will be different from this version once it has been copyedited and typeset.
PLEASE CITE THIS ARTICLE AS DOI: 10.1122/1.5000047

immediately after the first cycle, part of this energy dissipation is lost since the dissociation/reformation process of the reversible bonds does not occur instantaneously; a rest time must be imposed before the next tensile test in order to enhance the sample recovery and ensure a larger energy dissipation during the following loading/unloading cycle. For example, for the DDN studied by Jiang et al.,¹⁵ a maximum recovery was reached after 20 minutes of rest time. In a more general way, upon cyclic tensile tests, the beneficial effect of the supramolecular bonds on the mechanical properties of the DDN has been clearly demonstrated.¹⁰ However, it is highly dependent on the strain rate applied and on the ability of the reversible junctions to recombine during the experiments. Similar properties are also found with dual networks consisting of a single network containing both static and reversible crosslinks.^{26, 27} For example, it was shown by Wu et al.¹⁴ that a dual network based on covalent amide bonds and on hydrogen bonding between adjacent amide groups is generally more extensible than the two corresponding single networks.

From these examples, one can conclude that controlling the dynamics of the supramolecular network allows optimizing the network extensibility and toughness. However, these double dynamic networks formed by a static covalent and a supramolecular network have a main drawback: breakage of the covalent network will finally take place when increasing the deformation, and will lead to irreversible damage of the sample. A way to overcome this issue is to use two interpenetrated supramolecular networks with different dynamics. For example, through the incorporation of metal-ligand interactions of varying bond strengths,²⁸ we can imagine a new class of materials that have very high stretching capabilities and can self-heal at low temperatures. However, these fully supramolecular networks are susceptible to creep.

A further step in reducing the creep effect is to use networks with dynamic covalent bonds, which offer some dynamics while maintaining stability at longer timescales. A significant application of this concept can be found in vitrimers.²⁹ The dynamic covalent bonds are covalent bonds which can become dynamic in response to external stimuli such as temperature or pH. While under ordinary conditions, they behave as covalent static bonds and are able resist to creep, at high temperature or under the right stimulus, the bonds become dynamic and exchanges take place between neighboring dynamic bonds, enabling the sample to flow and/or self-heal. These networks, when combined with non-covalently bonded networks offer increased toughness, elasticity and self-healing properties.^{18, 19} Some of these materials are able to fully recover their mechanical properties after tensile testing, especially when two different types of dynamic covalent bonds are present.^{16, 17, 30}

Thus, double dynamic networks formed by a first, densely crosslinked network based on supramolecular junctions with short association/dissociation lifetimes, and by a second, loosely

This is the author's peer reviewed, accepted manuscript. However, the online version of record will be different from this version once it has been copyedited and typeset.
PLEASE CITE THIS ARTICLE AS DOI: 10.1122/1.5000473

crosslinked network based on slow dynamic covalent bonds seem very promising systems as they should allow combining toughness and extensibility at room temperature, while being fully self-healable and reprocessable at high temperature, at which the exchange dynamics of the covalent bonds occurs. However, obtaining these peculiar characteristics requires to precisely control the dynamics of the supramolecular network. In particular, the dissociation of the reversible junctions must occur during the sample deformation in order to have large extensibility, while their ability to create new junctions will affect the sample recovery.^{18, 19}

In the present work, we investigate the viscoelastic properties of such DDNs and study how the dynamics of the supramolecular network influences the equilibration and the creep-recovery properties of the dynamic covalent network. To this end, we synthesized a DDN in which the fast network is based on metallo-supramolecular junctions created from the complexation of Zinc(II) ions with pendant terpyridine groups placed along an unentangled poly(*n*-butyl acrylate) (*PnBA*),³¹⁻³³ while the second network consists of *PnBA* with pendant aldehyde groups and imine crosslinks. These two networks show very contrasting rheological behaviors as the association lifetimes of the two types of bonds, the sticker density, and the molecular weights of the polymer backbones are different by several orders of magnitude.

While the response of the metallo-supramolecular network can be tuned by changing the nature of the metal ion or the topology of the polymer building blocks, we focus here on investigating the influence of the temperature, the density of reversible junctions, and the stress applied on the viscoelastic properties. The reversible bonds, also referred to as “stickers”, can be in the open (unassociated) or closed state (associated).³⁴ For times shorter than the lifetime of the stickers, the supramolecular network behaves as a chemically crosslinked network, while at longer time, the stickers association/dissociation dynamics takes place, which allows the diffusion and the relaxation of the sticky chains, but with a delay when compared to the corresponding non-associated state.^{32, 35} Then, we would like to understand how modulating the dynamics of the metallo-supramolecular network affects the dynamics of the dynamic covalent network (DCN), and in particular, the ability of the latter to equilibrate locally, at the level of its network strands. This equilibration process should influence both the linear viscoelasticity and the creep-recovery properties^{36, 37} of the DDN.

The paper is organized as follows: In Section II, the materials and characterization methods are presented. In section III, the results obtained in the linear regime of deformation (see Section III.1) or by creep-recovery tests (see Section III.2) are presented and discussed, both for the single networks and for the double dynamics networks. Conclusions are drawn in Section IV.

II. Materials & Methods

II.1. Materials

Syntheses

Full details of the synthesis of the comonomers, the RAFT polymerization of the *PnBA*-co-PTPA copolymer (poly-*n*-butyl acrylate – co – terpyridine acrylate) and the free radical polymerization of the aldehyde copolymer are given in the supporting information (SI).

Their main characteristics of the copolymers and networks derived from them are given in Table 1. While a short, unentangled *PnBA* polymer (named *PnBA27k-7Tpy*) is used to build the metallo-supramolecular network, the dynamic covalent network is based on very long *PnBA* chains bearing aldehyde side groups (named *PnBA473k-18Ald*). The first number in the names of the copolymers represents the M_n of the copolymer, and the second number is the average number of terpyridine or aldehyde units in the copolymer. The metallo-supramolecular networks based on the terpyridine functionalized copolymers are named *PnBA27k-7Tpy-xeq*, where x ($x=0.5, 0.75$ or 1) is the number of added metal ions per terpyridine group. The dynamic covalent network based on the aldehyde functionalized copolymer is named *PnBA473k-18Ald-0.5eq*, indicating that only half of the aldehyde functions have been crosslinked.

Table 1. Structural Parameters of *PnBA* Polymers and Corresponding Single Networks

Sample	M_n (kg/mol) *	\bar{D}	Functional group	Functional groups/chain	Zn^{2+}/Tpy , imine/aldehyde molar ratio	T_g (°C)
<i>PnBA22k</i>	22	1.19	/	-	/	-48
<i>PnBA27k-7Tpy</i>	27	1.18	Tpy	7	0	-48
<i>PnBA27k-7Tpy-0.5eq</i>	27	1.18	Tpy	7	0.5 eq.	-45
<i>PnBA27k-7Tpy-0.75eq</i>	27	1.18	Tpy	7	0.75 eq.	-48
<i>PnBA27k-7Tpy-1eq</i>	27	1.18	Tpy	7	1 eq.	-46
<i>PnBA473k-18Ald</i>	473	1.94	Aldehyde	18	0	-47
<i>PnBA473k-18Ald-0.5eq</i>	473	1.94	Aldehyde	18	0.5 eq.	

* M_n from GPC measurement using a PS calibration, Tpy=terpyridine, Ald=aldehyde

Preparation of Metallo-Supramolecular Networks

The gels were prepared by dissolving 100 mg of the *PnBA-co-PTPA* copolymer in 100 μ L of acetone in a vial. Then, the vial was shaken to homogenize the concentrated solution. The metal containing solution was obtained by dissolving the corresponding salt in methanol at a concentration of around 10-20 mg/mL. The solution containing the transition metal was subsequently added to the polymer vial to reach a 0.5, 0.75 or 1 molar ratio between metal ions and terpyridine. Finally, the vial was shaken again to ensure total complexation of the metal, followed by solvent evaporation under vacuum to obtain a homogenous transient polymer network. The different metallo-supramolecular networks are listed in Table 1.

Preparation of Imine-Aldehyde Networks

150 mg of the benzaldehyde-functionalized *PnBA* polymer were first dissolved in 0.1 mL of THF in a small glass vial. Next, the amount of imine solution (at a concentration of ca. 10 mg/mL) required to crosslink 50% of the available benzaldehyde groups is added, and the vial is shaken to mix all components. The solution is then poured into an 8 mm circular Teflon mold, covered loosely and left to air-dry for 3 days. Finally, the mold is placed into a vacuum oven and dried at 110°C overnight.

Preparation of Double Dynamic Networks

50 mg of the benzaldehyde-functionalized *PnBA* polymer and 120 mg of the *PnBA-co-PTPA* copolymer were first dissolved in 0.3 mL of THF in a small glass vial. To this, the amount of imine solution (at a concentration of ca. 10 mg/mL) required to crosslink 50% of the available benzaldehyde groups were added. Next the amount of Zn^{2+} solution (concentration ca. 20 mg/mL of $ZnCl_2$) required to crosslink all the available terpyridine groups (Zn/Tpy ratio of 0.5), were added and the vial is shaken to mix all components. The solution was then poured into an 8 mm circular Teflon mold, covered loosely, and left to air-dry for 3 days. Finally, the mold was placed into a vacuum oven and dried at 110°C overnight. Figure 1 illustrates the single and double dynamic networks obtained.

This is the author's peer reviewed, accepted manuscript. However, the online version of record will be different from this version once it has been copyedited and typeset.
PLEASE CITE THIS ARTICLE AS DOI: 10.1122/1.5000473

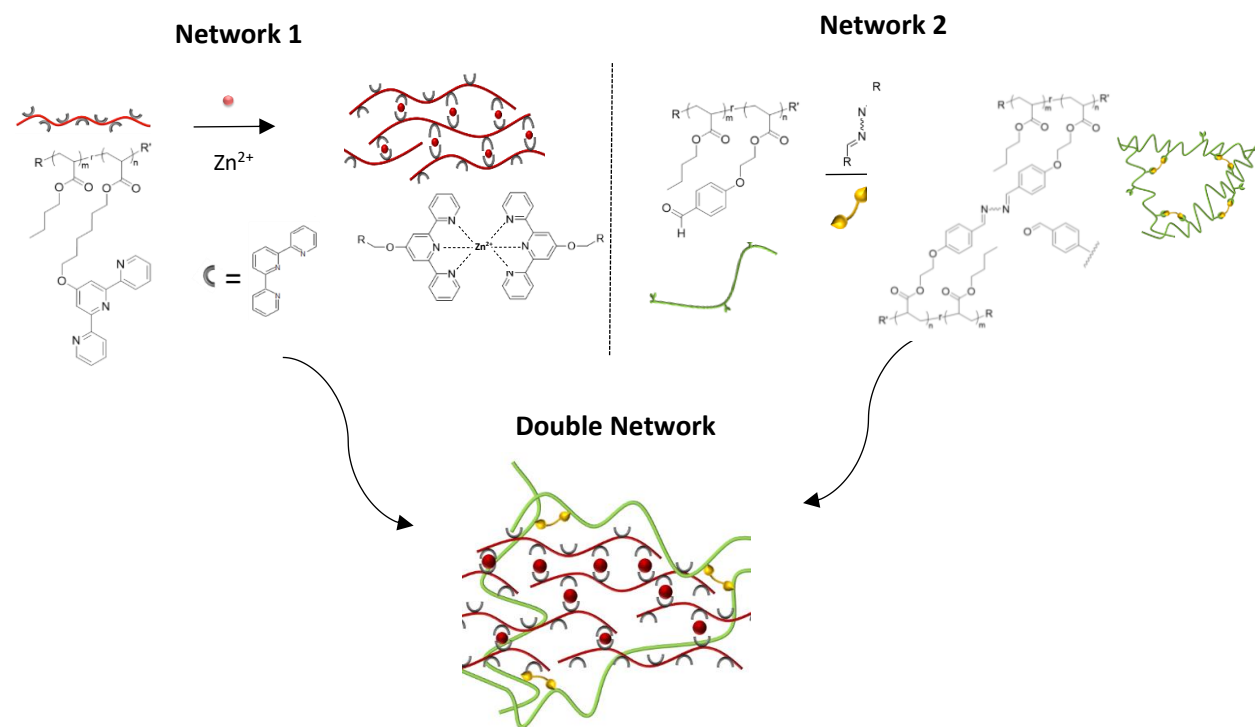


Figure 1: Summary of the syntheses of Network 1 and Network 2, and schematic representation of the double dynamic network

II.2. Measurements

Shear rheology experiments were performed on the ARES G2 rheometer with 8 mm parallel plates and the temperature was controlled by the convection oven under nitrogen atmosphere. All samples have been characterized at temperatures ranging from $-20\text{ }^{\circ}\text{C}$ to $100\text{ }^{\circ}\text{C}$. Firstly, samples were equilibrated at $130\text{ }^{\circ}\text{C}$ for 15 minutes, then the temperature was lowered to the highest measuring temperature, where the sample was left to settle again for 15 minutes. A strain sweep was then performed at 10 rad/s , stopping before the crossover point is reached, followed by a frequency sweep at an appropriate strain value in the linear range between 200 rad/s and 0.01 rad/s . The frequency sweep was repeated at intervals of at least 30 minutes to ensure repeatability of the measurement. This procedure was repeated for the next highest measuring temperature, and so on up to $-20\text{ }^{\circ}\text{C}$. The master-curves were then built at a reference temperature of $25\text{ }^{\circ}\text{C}$, as detailed in Section III.1.

Creep measurements were performed on the stress-controlled Anton Paar MCR 51 rheometer. The samples were first equilibrated at $130\text{ }^{\circ}\text{C}$ for 15 minutes, then cooled to $25\text{ }^{\circ}\text{C}$. A strain sweep was performed at 10 rad/s as previously described to determine the linear regime. The creep measurements were then performed according to the following protocol: a given shear stress (10, 100,

This is the author's peer reviewed, accepted manuscript. However, the online version of record will be different from this version once it has been copyedited and typeset.
PLEASE CITE THIS ARTICLE AS DOI: 10.1122/1.50000473

500 or 1000Pa) was applied for 30 minutes at 25 °C and then set to 0 Pa. After a first recovery period of 30 min at 25°C, the temperature was raised to another temperature (40 °C, 50 °C, 60 °C or 80 °C in Figure 11; 40 °C or 80 °C in Figures 12-14) and kept for 30 min. Then, temperature was raised and kept by steps of 20 °C for every 30 min until the equilibrium temperature for the first network was reached (130 °C) or until the complete recovery of the sample. The sample was left at 130 °C for 30 minutes, cooled to 25 °C and a frequency sweep performed to ensure non-degradation of the sample. This entire procedure was then repeated for each value of applied stress.

III. Results and Discussion

In this section, the linear rheology of the two separate polymer networks, and then of the double dynamic networks, is presented. Based on these results, the creep-recovery properties of these samples are presented and analyzed.

III.1. Linear Viscoelastic Properties (LVE)

A. LVE of the Metallo-Supramolecular Network

The first network is based on a linear *Pn*BA $M_n=27$ kg/mol which contains 7 pendant terpyridine groups per chain in average (see Table 1). Its viscoelastic response was studied as a function of temperature and with varying amounts of zinc ions (see Table 1): a stoichiometric ratio of ions, which corresponds to 0.5 equivalent (eq.) of ions per equivalent of terpyridine ligand, or with an excess amount of ions (0.75eq. and 1 eq.). Figure 2 presents a summary of their rheological behavior between -20 °C and 60 °C.

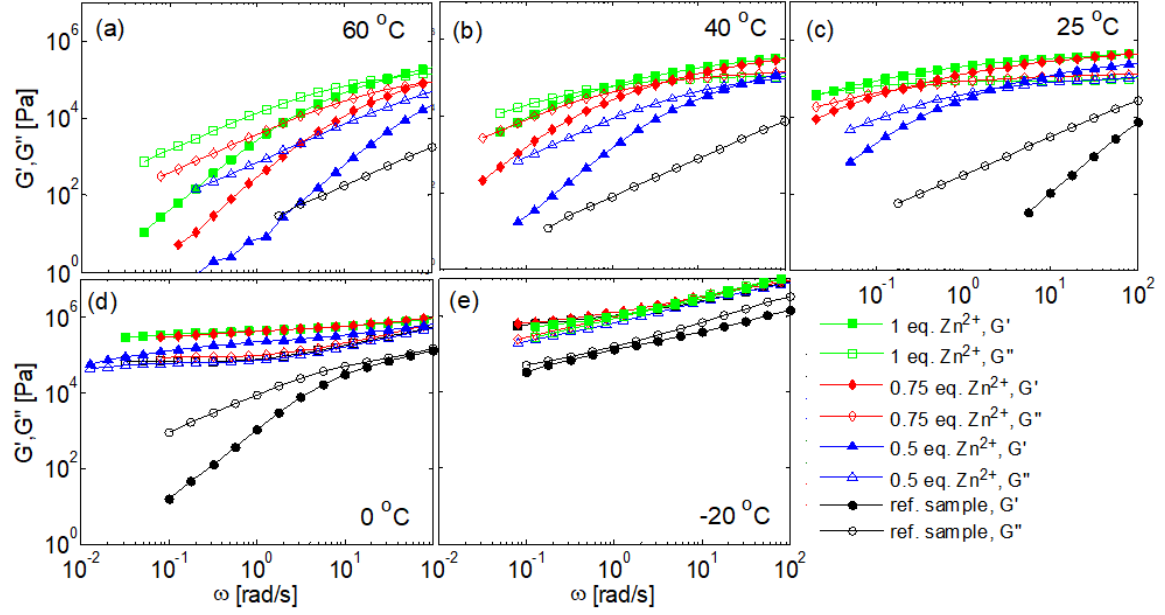


Figure 2: Frequency sweeps at temperatures ranging from 60 °C to -20 °C for sample PnBA27k-7Tpy in the presence of 0 to 1 equivalent of Zn^{2+} ions. The loss modulus of the reference sample is not shown at high temperature as it could not be correctly measured due to a too weak torque signal.

For all temperatures, the reference polymer (Figure 2, black symbols) relaxes faster than the metallo-supramolecular networks. Since the average molar mass between two entanglements, M_e , for the PnBA is equal to 18 kg/mol,³⁸ the reference sample is essentially unentangled, with no sign of a rubbery plateau. Its relaxation should follow a Rouse relaxation process, taking place between its glassy regime and its terminal regime. The influence of temperature can therefore be taken into account by the Williams-Landel-Ferry (WLF) equation:

$$\log_{10} a_T = \frac{-c_1^0 (T - T_{ref})}{c_2^0 + (T - T_{ref})}, \quad (1)$$

where the c_1 and c_2 constants have been fixed to $c_1^0 = 6.2$ and $c_2^0 = 131.17$ K at a reference temperature, T_{ref} , of 25 °C.³⁹ In addition, a vertical shift factor, $b_T = \frac{\rho_{ref} T_{ref}}{\rho T}$, with the density $\rho = (1.2571 - 6.89 \cdot 10^{-4} T) \text{ g/cm}^3$, has been applied in order to account for the temperature dependence of the sample density and elasticity.⁴⁰ The master-curve obtained with these shift factors is presented in Figure 3a. The experimental data are compared to the theoretical curves predicted by assuming that the reference sample relaxes through a Rouse process:⁴¹

$$G_{Rouse}(t) = \sum_i v_i \frac{\rho R T}{M_{w,i}} \sum_{p=1}^{\infty} \exp\left(-\frac{2p^2 t}{\tau_R(M_i)}\right) = \frac{5}{4} G_N^0 \sum_i v_i \frac{M_e}{M_{w,i}} \sum_{p=1}^{\infty} \exp\left(-\frac{2p^2 t}{\tau_R(M_i)}\right), \quad (2)$$

where τ_R is the Rouse relaxation time of the chains and was fixed to $2 \cdot 10^{-3}$ s by best-fitting procedure. Its value corresponds to the inverse frequency at which the viscoelastic modes of Rouse relaxation

ends and the terminal regime starts, ρ is the polymer density and G_N^0 , the plateau modulus of an entangled PnBA polymer (=160 kPa, see ref. ³⁸), and v_i is the weight fraction of chains with mass M_i . The molar mass dispersity was accounted for assuming a log-normal molar mass distribution with $M_n=27$ kg/mol and a molar mass dispersity of 1.2 (see Table 1). The storage and loss moduli of the sample were determined from the relaxation modulus, using the Schwarzl approximations.⁴² An overall good agreement is obtained between the experimental and predicted data.

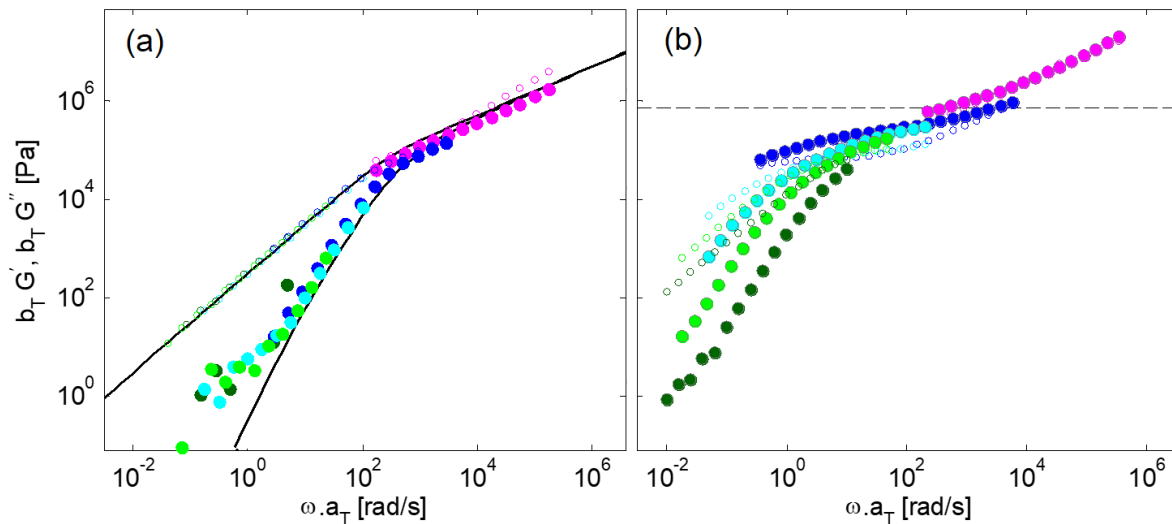


Figure 3: Master curves of the storage (filled symbols) and loss (empty symbols) moduli for a), the reference sample PnBA27k-7Tpy and b) PnBA27k-7Tpy-0.5eq, at the reference temperature of 25 °C. The dashed line represents the hypothetical level of the rubbery plateau if all the bis-complexes were formed. The data have been measured at -20 °C (magenta), 0 °C (blue), 25 °C (cyan), 40 °C (green) and 60 °C (dark green).

As shown in Figure 3b for sample PnBA27k-7Tpy-0.5eq, using the WLF equation to shift the viscoelastic data of the metallo-supramolecular networks does not allow building a master-curve. In these data, we see the emergence of a rubbery plateau, which is attributed to the presence of the reversible crosslinks. Assuming a perfect network in which all the bis-complexes are formed, the theoretical value of the rubbery plateau would be provided by the following formula:

$$G_{N,tpy}^0 = \frac{\rho RT}{M_{xx}}, \quad (3)$$

where M_{xx} is the average molar mass between two stickers ($M_{xx}=4$ kg/mol). It corresponds to the dashed line in Figure 3b. A storage modulus larger than this value indicates that the molecular sub-chains shorter than M_{xx} are not relaxed yet. Since the relaxation of these sub-chains does not require the dissociation of the stickers, we would expect that, at this length scale, the dynamics of the metallo-

supramolecular network is similar to the one of the reference sample (knowing that the glass transition temperature does not vary with the addition of metal ions). However, the influence of the metal ions is already visible, as also evidenced by the un-shifted data presented in Figure 2e. This suggests that the local dynamics of the sticky chains is affected even at a shorter length scale, close to the length scale of a Kuhn segment (of length 2.29nm and mass 1190 g/mol).⁴³

In order to relax, the supramolecular crosslinks have to dissociate and re-associate several times, to allow the whole chain to move and renew its configuration. According to the sticky Rouse model,³⁵ the terminal relaxation time of such unentangled sticky chains depends on the time $\tau_{sticker}$, i.e., the time that a sticker needs to change partner, and on the number of stickers per chain $N_{sticker}$, and is equal to $\tau_{sticker}N_{stickers}^2$. While the number of stickers per chain is fixed from the synthesis, their average lifetime is unknown. It has been shown in previous works that the latter strongly depends on temperature and should follow an Arrhenius equation:⁴⁴⁻⁴⁶

$$\tau_{sticker} \propto \tau_l \exp\left(\frac{E_a}{k_B T}\right), \quad (4)$$

where τ_l is a local attempt time, E_a the activation energy of $\tau_{sticker}$, and k_B the Boltzmann constant. As τ_l depends on the chain mobility at a local level, it has the same temperature dependence as the Rouse relaxation time of a Kuhn segment, or, equivalently, as the non-crosslinked PnBA sample. Consequently, its temperature dependence is well described by the WLF equation (see eq. 1). Thus, in order to build a master-curve for the metallo-supramolecular networks, one should use the following horizontal shift factors:

$$a'_T = a_T \exp\left(\frac{E_a}{R} \left(\frac{1}{T} - \frac{1}{T_{ref}}\right)\right), \quad (5)$$

where R is the gas constant and T_{ref} is fixed to 298K. The unknown activation energy of $\tau_{sticker}$ is found by best-fitting procedure. Results are shown in Figure 4 for the different metallo-supramolecular networks, considering that the sticker activation energy, E_a , is equal to 40 kJ/mol. The latter value depends on the association energy of the metal-ligand complexes, but also on the number of times a sticker has to dissociate and associate before changing partners.⁴⁶ Consequently, E_a also depends on the crosslink density and on the network topology. The E_a values for other metallo-supramolecular networks based on zinc-terpyridine complexes were already determined. For example, a E_a of 81kJ/mol was estimated for a 4-armed telechelic star polymer melt ($M_n = 250\text{kg/mol}$) crosslinked with Zn^{2+} ions,³² or a E_a of 30kJ/mol was found in the case of telechelic tetra-PEG hydrogels ($M_n = 20\text{kg/mol}$).⁴⁷ The responses of the different metallo-supramolecular networks are compared to the viscoelastic data of the reference sample in Figure 4d. The use of Equation 5 yields a good superposition of the curves

at high and intermediate frequency. However, a significant discrepancy appears between the curves at low frequencies, at which the sample shows a complex thermo-rheological behavior. It must be noted here that we could have fixed the activation energy to other values in order to optimize the superposition of the moduli at low frequency, however this approach is not appropriate for two reasons at least. First, data shifted in such a way do not superimpose well at low frequency since the shape of the storage and loss moduli curves are temperature dependent, which cannot be corrected by a simple horizontal shift of the data. The second reason is that in the low frequency region, the values of the storage modulus are low, and in particular they are lower than the modulus corresponding to the longest mode of the Rouse relaxation, $\frac{\rho RT}{M_w}$ (see Equation 2), represented by the dashed-dotted line in Figure 4. Therefore, in this regime, the gradual relaxation of the sub-chains from the level of the strands localized between two stickers up to the level of the whole chain, which takes place from a modulus of $G'_{tpy} = \frac{\rho RT}{M_{XX}}$ (dashed line) down to the value $G'_1 = \frac{\rho RT}{M_w}$ (dashed-dotted line), already happened. Hence, it seems better from a physical point of view to fix E_a to ensure building a good master-curve in the intermediate regime, since it is in the latter that the sticker dynamics is expected to be dominant.

The thermo-rheological complexity observed at low frequency is not expected if we consider that the samples relax by a sticky Rouse process. Indeed, according to this model, the Rouse modes of the sticky chains, which involve the association/dissociation of the stickers, should be delayed by a constant factor which depends on the sticker lifetime, and thus, on the temperature. Here, we observe that a decrease of the temperature leads to a broader relaxation time spectrum, and this effect is more pronounced when larger amounts of ions are added. We attribute it to the presence of inter-chain entanglements. Indeed, with a weight average molar mass of 32 kg/mol, a molar mass dispersity of 1.18, and an average molar mass between two entanglements equal to 18 kg/mol,³² some of the chains have a molar mass above $2M_e$ and thus, are potentially entangled. While for the reference sample the influence of these entanglements is negligible thanks to the dilution effect of the shorter chains, this is not the case anymore with sticky chains, which are moving in a denser network with a mesh-size of around 4 kg/mol (see Table 1). In order to disentangle, the whole chain has to diffuse, which requires a concerted action of all the stickers of its backbone. Therefore, the corresponding disentanglement time is expected to be longer than the sticky Rouse relaxation time. In addition to depending on the number of stickers per chain and on their lifetime, the chain diffusion also depends on the average proportion of associated stickers in the sample as this will determine the proportion of entanglements trapped in the network.³⁸ Since these variables do not have the same temperature-dependence, thermo-rheological complexity is therefore expected.

This is the author's peer reviewed, accepted manuscript. However, the online version of record will be different from this version once it has been copyedited and typeset.
PLEASE CITE THIS ARTICLE AS DOI: 10.1122/1.5000047

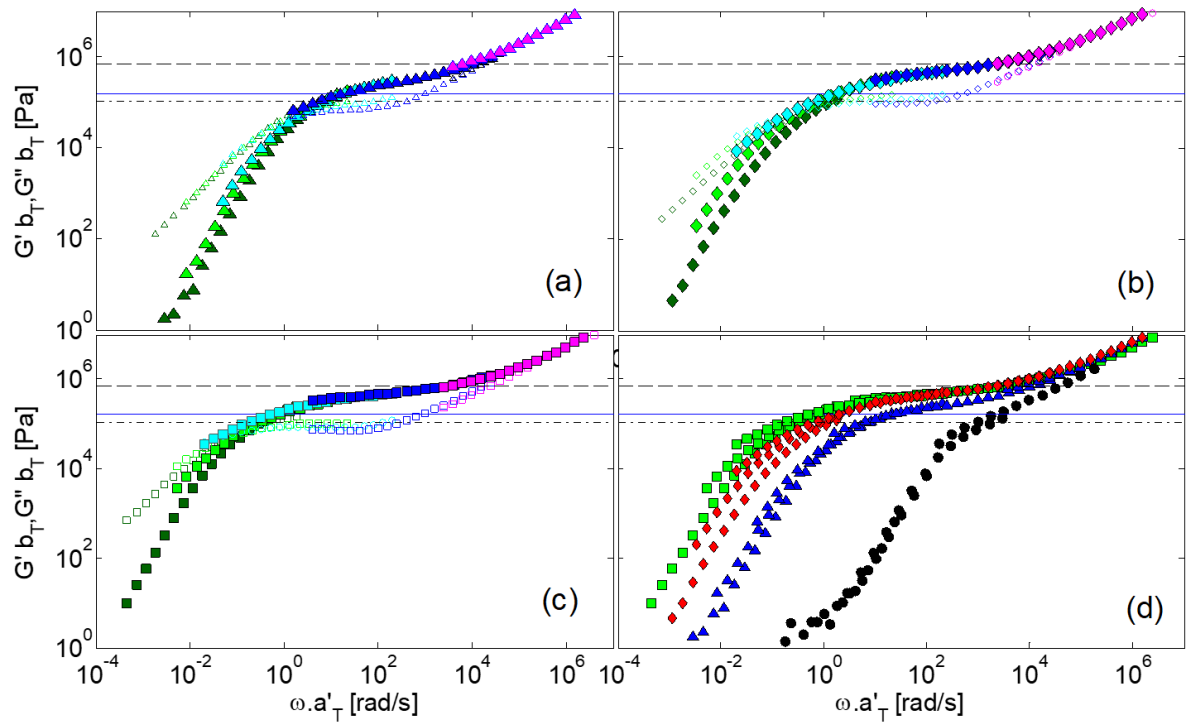


Figure 4: Master curves of the storage (filled symbols) and loss (empty symbols) moduli of (a) PnBA27k-7Tpy-0.5eq (Δ), (b) PnBA27k-7Tpy-0.75eq (\diamond), and (c) PnBA27k-7Tpy-1eq (\square), built with Equation 5 and $E_a = 40\text{kJ/mol}$, at reference temperature $T_{ref} = 25\text{ }^\circ\text{C}$. The data have been measured at $-20\text{ }^\circ\text{C}$ (magenta), $0\text{ }^\circ\text{C}$ (blue), $25\text{ }^\circ\text{C}$ (cyan), $40\text{ }^\circ\text{C}$ (green) and $60\text{ }^\circ\text{C}$ (dark green). d) The storage moduli of the metallo-supramolecular networks containing 0.5eq. (\diamond), 0.75 eq. (\square) or 1 eq. (Δ) of Zn^{2+} are compared to the one of the reference sample PnBA27k-7Tpy (o). The dashed line represents the level of the rubbery plateau if all the stickers were associated; the dashed-dotted line represents the contribution of the longest Rouse mode, $\frac{\rho RT}{M_w}$ (see Eq. 2), and the blue line represents the entanglement plateau modulus (160 kPa).

Furthermore, according to the sticky Rouse model, the storage and loss moduli should decrease with a slope of $\frac{1}{2}$ in the intermediate regime at which the different modes of the sticky Rouse process are gradually relaxing. This is not observed here; going down to lower frequency, the storage modulus rather decreases smoothly, with a slope of around 0.15, until it reaches the relaxation of the entire chain (at the level of the dashed-dotted line). This is better seen in Figure 5, in which the storage moduli of the metallo-supramolecular networks and of the reference sample are horizontally shifted in order to show the same terminal regime. The shift factors are shown in the inset figure. One can clearly see that the reference sample is the only sample relaxing by Rouse until its terminal regime is reached. For all the metallo-supramolecular networks, the Rouse relaxation stops as soon as the strands of mass M_{xx} are relaxed (for G' at the level of the dashed line). Here again, a possible explanation for this different behavior is the fact that the sample is at the limit to be entangled ($M_e = 18\text{ kg/mol}$), which is

This is the author's peer reviewed, accepted manuscript. However, the online version of record will be different from this version once it has been copyedited and typeset.
PLEASE CITE THIS ARTICLE AS DOI: 10.1122/1.5000047

expected to strongly affect the sample relaxation. In particular, the supramolecular assemblies created by the formation of bis-complexes are certainly entangled. For comparison, the level of the plateau modulus of an entangled PnBA polymer is shown in Figure 4 (see blue line). The possible contribution of the entanglements cannot be considered as negligible compared to the contribution of the stickers. Finally, the higher level of the rubbery plateau found with larger amounts of Zn²⁺ ions (see Figure 4d) suggests that in average, the chains contain a larger number of associated stickers, i.e., the network is more densely crosslinked when a larger amount of ions is added. This result is in agreement with ref. ³⁹, where it was found that with a metallo-supramolecular network formed by telechelic star polymers in the melt state, the probability for a sticker to be free is decreasing while increasing the amount of ions slightly above its stoichiometric amount. It differs, however, from the metallo-supramolecular gels,^{48, 49} where zinc-terpyridine mono-complexes are favored at over-stoichiometric proportion of ions.

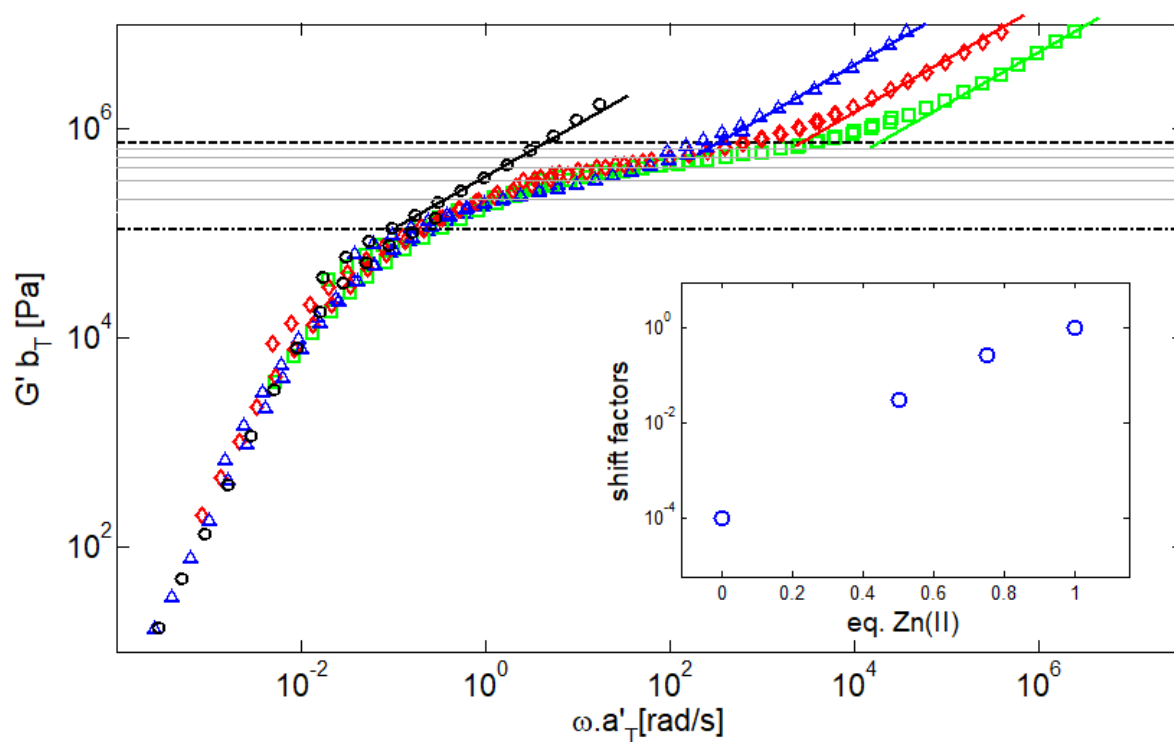


Figure 5: Storage moduli of the reference sample and of metallo-supramolecular networks containing 0.5 eq. (Δ), 0.75 eq. (\diamond), and 1 eq. (\square) of ions. The master-curves have been built with Equation 5 and $E_a = 40$ kJ/mol at $T_{ref} = 25$ °C, and then horizontally shifted by a factor of 1.10^{-4} , 3.10^{-2} , $2.5.10^{-2}$ and 1 (see inset), respectively. The dashed line represents the level of the rubbery plateau if all the stickers are

associated; the dashed-dotted line represents the contribution of the longest Rouse mode, $\frac{\rho RT}{M_w}$ (see Eq. 2). The thin grey lines represent the level of the modulus if 2,3,..., N_{st} Rouse modes are not relaxed.

B. LVE of the Dynamic Covalent Network

The second network is made of PnBA chains with a M_n of 473 kg/mol. These polymer chains bear 18 aldehyde side groups in average, of which half were turned into dynamic imine crosslinks (see Table 1, sample *PnBA473k-18Ald-0.5eq*). As shown in Figure 6a, the master-curve obtained for the reference polymer and the WLF equation (see Equation 1) shows a rubbery plateau due to the presence of entanglements. At low frequency, the cross-over between the storage and loss moduli, which is associated to the solid-to-liquid transition of the sample, is observed. However, the terminal regime is not yet fully reached at 100 °C as the terminal slopes of G' and G'' are not equal to 2 and 1.

When the crosslinker is added, dynamic covalent crosslinks are formed. In the range of temperatures and frequencies investigated, it is expected that these bonds are stable, and therefore, behave similarly as static covalent bonds. This is confirmed by the appearance of a second, low frequency plateau (Figure 6a), which is attributed to the entanglements trapped between two crosslinks and which are unable to relax.³⁸ The static behavior of the crosslinks is also confirmed by the thermo-rheological simplicity of the data, the master-curve being only built based on the WLF equation. As the crosslink density is rather low (corresponding to a weight-average molar mass of 100 kg/mol between two crosslinks), the dynamic covalent network (DCN) contains a large proportion of dangling ends. The relaxation of the latter is observed at intermediate frequencies.

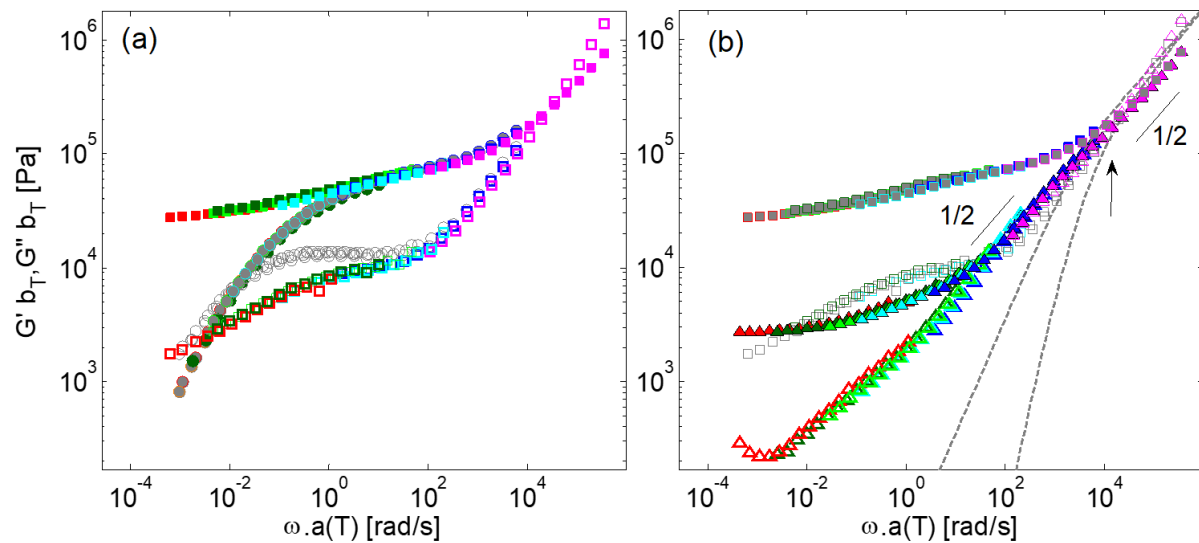


Figure 6: (a) Master-curves of the storage (filled symbols) and loss (empty symbols) moduli of the reference polymer PnBA473k-18Ald (grey, o) and of the imine-aldehyde network PnBA473k-18Ald-0.5eq (color, □), at $T_{ref}=25$ °C. The data have been measured at -20 °C (magenta), 0 °C (blue), 25 °C (cyan), 40 °C (green), 60 °C (dark green), and 80 °C (orange) and 100 °C (red). (b) Master-curves of the imine-aldehyde network PnBA473k-18Ald-0.5eq, pure (grey, □) or diluted at 30 wt% in a matrix of short PnBA chains of molar mass of 22 kg/mol (color, Δ). The theoretical Rouse relaxation of PnBA22k is also shown (dashed curves). The arrow indicates the relaxation of the short chains.

The dynamic covalent network was then diluted at a concentration of $v_{DCN} = 30$ wt% in a matrix of short ($M_n = 22$ kg/mol) PnBA chains. This concentration was chosen as low as possible while ensuring the formation of a stable network (see SI, Figure S11). As shown in Figure 6b, this lowers the second, low frequency, plateau of the dynamic covalent network, which is vertically shifted by a factor equal to $v_{DCN}^2 = 0.09$, due to both the dilution of the network and to the increase of the molar mass of the effective entanglement segments,⁵⁰ from M_e to $\frac{M_e}{v_{DCN}}$. As the short chains are mostly unentangled, they relax at very high frequency, as indicated by the arrow. While at long times they act as a solvent for the network, at intermediate times they govern the local reorganization of the network which takes place at the level of an entanglement segment up to the level of a molecular strand localized between two dynamic covalent crosslinks. In this intermediate regime, as further described in Part C, the strands of the DCN equilibrate by a Constraint Release Rouse (CRR) process at the rhythm of the short chain motions.⁵¹

C. LVE of the Double Dynamic Networks

The double dynamic networks (DDN) are composed of 30 wt% of the stable dynamic covalent network diluted in the metallo-supramolecular network, with different amounts of Zn^{2+} ions. Figure 7 presents the viscoelastic data of the DDN containing 0.5 eq. or 0.75 eq. of Zinc ions. It is seen in Figures 7a and 7c that applying the WLF equation (see Equation 1) to the curves measured at different temperatures does not allow building a master-curve. In particular, a large discrepancy is observed at intermediate frequencies.

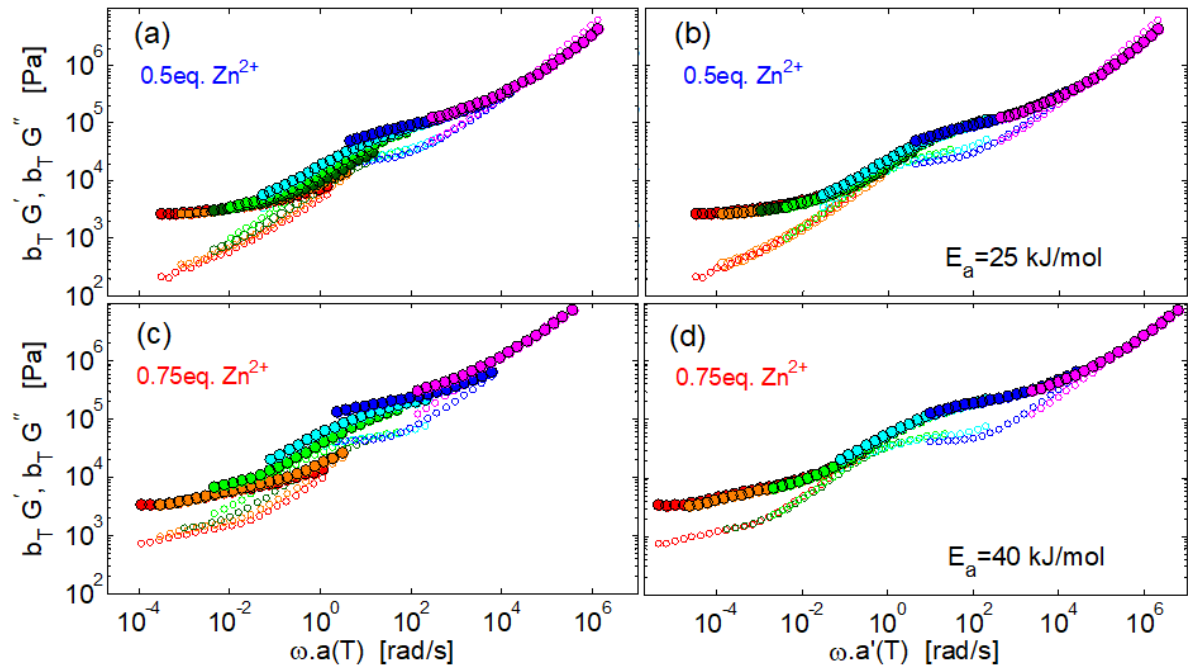


Figure 7: Master-curves of the storage (filled symbols) and loss (empty symbols) moduli for the DDN containing 0.5 eq. or 0.75 eq. of Zn^{2+} ions added to the first network, at $T_{ref} = 25^\circ C$. (a) The data have been measured at $-20^\circ C$ (magenta), $0^\circ C$ (blue), $25^\circ C$ (cyan), $40^\circ C$ (green), $60^\circ C$ (dark green), and $80^\circ C$ (orange) and $100^\circ C$ (red) and have been shifted either by the WLF equation (a and c), or according to Equation 5 (b and d).

In this regime, the DCN partially relaxes by CRR process. As illustrated in Figure 8, after the high frequency Rouse relaxation, the DCN is moving in a dense network mostly governed by the metallo-supramolecular crosslinks. This leads to the appearance of a plateau, the level of which strongly depends on the average density of associated stickers. However, at times longer than the lifetime of the bis-complexes, the stickers continuously dissociate and re-associate, and the sticky chains begin to relax. This allows the DCN to locally move and relax longer and longer molecular segments, of mass M_{xx} up to the relaxation of segments of mass M_e/u_{DCN} , which corresponds to the level of the low frequency plateau. Thus, this Constraint Release Rouse relaxation (with a characteristic slope of $\frac{1}{2}$ for G' and G'') is dictated by the dynamics of the metallo-supramolecular network, and in particular by the time that a sticky chain needs to diffuse, allowing the DCN to further explore its surrounding (see Figure 8). Therefore, its temperature dependence should follow an Arrhenius behavior. This is confirmed in Figures 7b and 7d, which show that by shifting the data with Equation 5, a good superposition of the viscoelastic curves is obtained in the frequency range governed by the sticker dynamics. The corresponding activation energy of the stickers, which has been determined by best-fitting procedure,

has been fixed to 25 kJ/mol and 40 kJ/mol for the DDN containing 0.5eq. or 0.75 of ions, respectively. While with 0.75 eq. of ions, E_0 is the same as the for the single metallo-supramolecular networks (see Part A), a lower value is found with 0.5eq. of ions. This weaker influence of temperature can also be seen by comparing the importance of the Time-Temperature Superposition failure in Figures 7a and 7c. We attribute it to the large fraction of dangling ends present in this system, as confirmed in Figure 9, where the plateau modulus of the DDN containing 0.5 eq. of ions is much lower than with 0.75eq. of ions and is at the level of the entanglement plateau (160 kPa). This suggests that the probability of having unassociated stickers in this sample is very large.

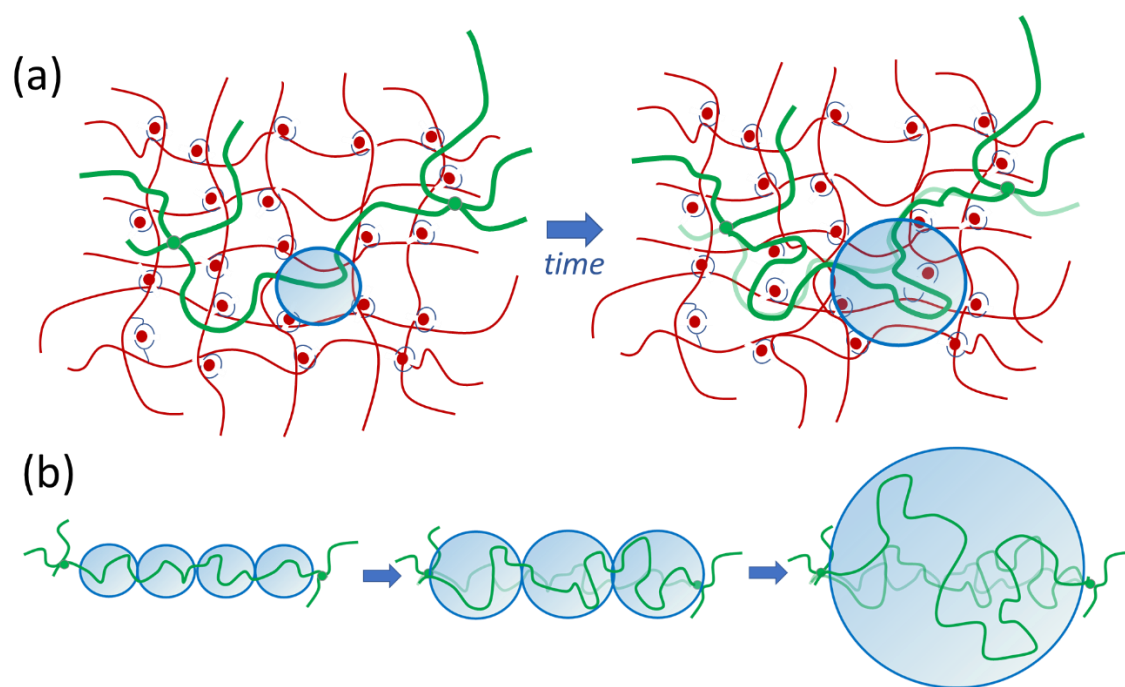


Figure 8: Cartoon illustrating the Constraint Release Rouse relaxation of the dynamic covalent network due to the relaxation of the metallo-supramolecular network. (a) At short time, the local motions of DCN are constrained by the metallo-supramolecular network ($M_{xx} = 4 \text{ kg/mol}$). However, with time, the bis-complexes dissociate and associate again and the sticky chains relax, allowing the DCN to explore a larger space (represented by the blob). (b) Schematic representation of the CR Rouse relaxation of the crosslinked strands of the DCN, from blobs of mass M_{xx} to blobs of mass M_e/ν_{DCN} .

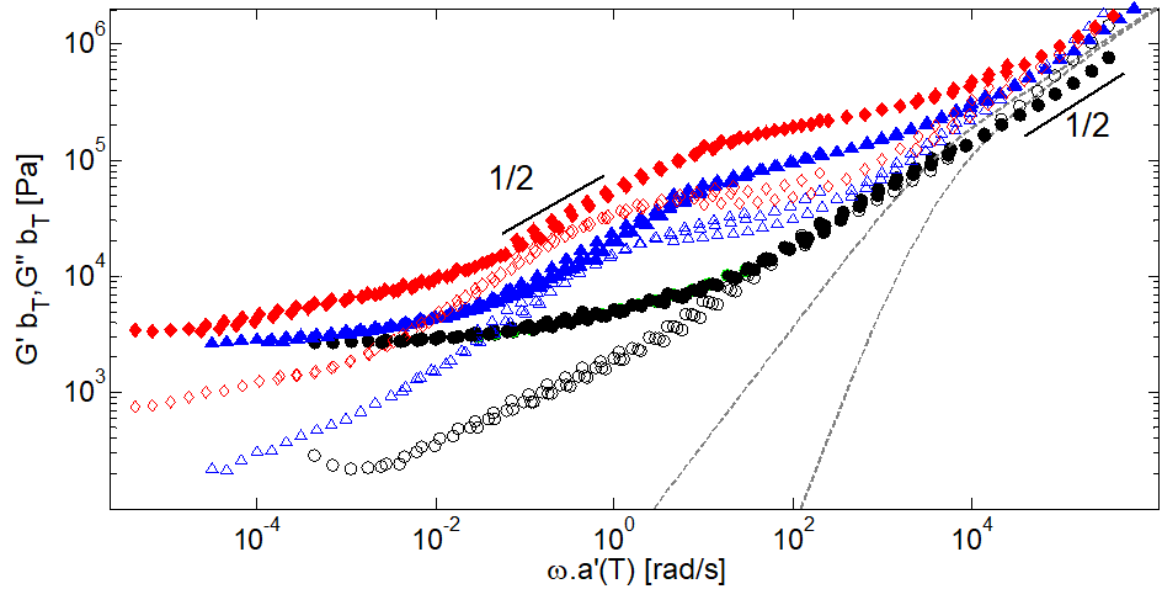


Figure 9: Master curve of the storage (filled symbols) and loss (empty symbols) moduli for the double dynamic network containing 0.5 eq. (blue Δ) or 0.75 eq. (red \diamond) of Zn^{2+} ions, compared to the DCN diluted in a short chain matrix PnBA22k (black o), at $T_{ref} = 25$ °C. The dashed curves represent the theoretical data of PnBA22k.

We may then conclude that the CRR regime can be controlled by varying the amount of Zn^{2+} ions, which governs the relaxation of the metallo-supramolecular network. This is well illustrated in Figure 9, where it is seen that the local equilibration of the DCN segments of mass M_e/ν_{DCN} is delayed, compared to their equilibration when the DCN is diluted in the short chain matrix PnBA22k. The delay factors observed in the CRR region of these different samples are the same as those used to superimpose the terminal regime of the single networks (see the inset of Figure 5), supporting our hypothesis that, indeed, the relaxation of the metallo-supramolecular chains fully governs the equilibration of the crosslinked strands of the DCN.

The role of the metallo-supramolecular network on the CRR relaxation of the DCN is also shown in Figure 10, where the CRR relaxation of the DCN starts at the relaxation time of the corresponding single metallo-supramolecular networks. While the similitude between the responses of the DDN and of the metallo-supramolecular networks at intermediate and high frequency is evident, we must note however that in order to obtain a good superposition of the data, the experimental data of the single networks have been shifted vertically by a factor 4/9. This is partially due to the lower number of reversible crosslinks present in the DDN since the latter contain 70% of the densely crosslinked metallo-supramolecular network. Its contribution to the plateau modulus is thus expected to be around 2/3 of its initial value. The larger dilution effect suggests that the mesh-size of the DDN is also

This is the author's peer reviewed, accepted manuscript. However, the online version of record will be different from this version once it has been copyedited and typeset.
PLEASE CITE THIS ARTICLE AS DOI: 10.1122/1.5000047

increasing, by a factor of around 3/2, compared to the corresponding single metallo-supramolecular network.

After the CRR relaxation, the storage modulus of the DDN containing 0.75 eq. of Zn^{2+} ions first slightly decreases (in the frequency range from 10^{-2} to 10^{-4} rad/s), before reaching its low frequency plateau (Figure 10). While the origin of this slow relaxation process is not clear, it could be due to the partial entanglement of the sticky chains, which delays their relaxation, and thus, the rhythm at which the DCN relaxes by CRR process. As discussed in Part A of this section, this partial entanglement of the chains is also at the origin of the thermo-rheological complexity observed in the data of the metallo-supramolecular network.

To conclude, as further detailed in Section III.2, varying the dynamics of the metallo-supramolecular network allows us to control the equilibration process of the DCN. This is of interest as it should also control how fast the DCN will be able to recover its initial shape after a large deformation.

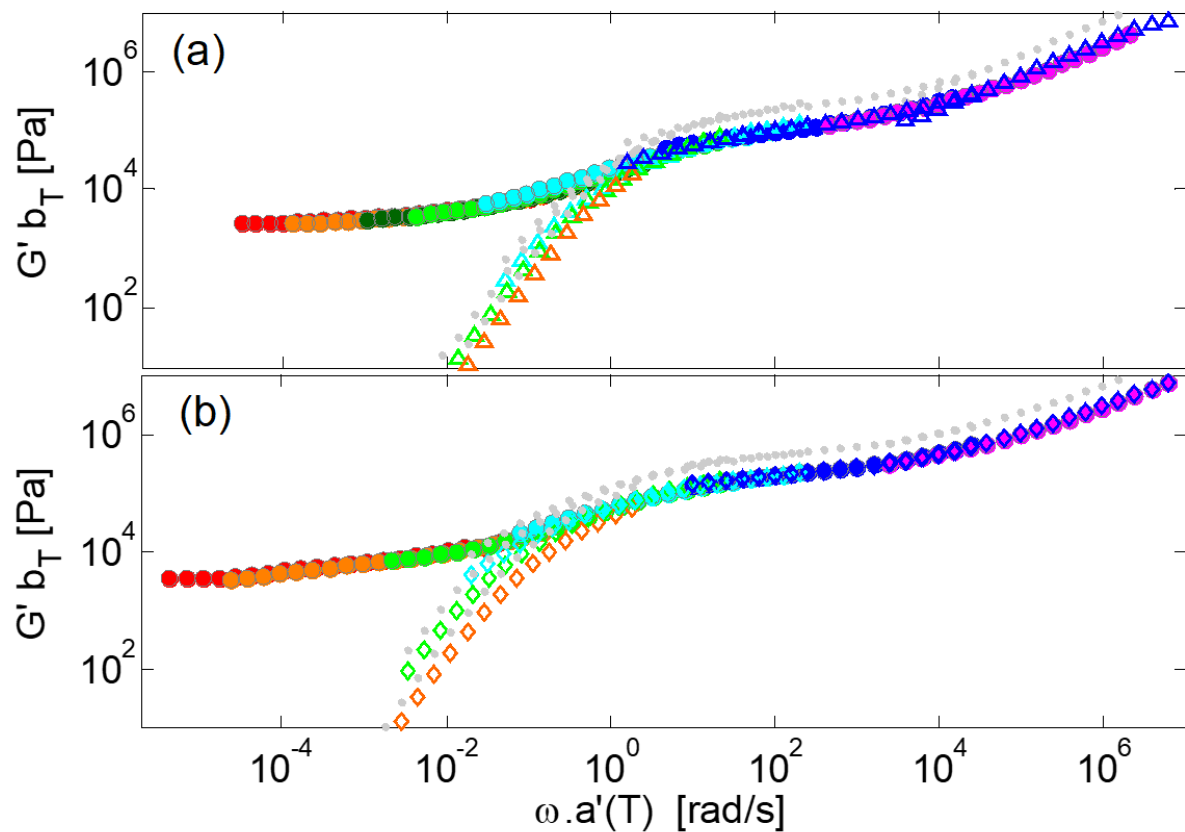


Figure 10: Comparison between the storage moduli of the double dynamics networks (o) containing 0.5 eq. (a) and 0.75 eq. (b) of Zn^{2+} ions with their corresponding single metallo-supramolecular networks (Δ) at a reference temperature $T_{ref} = 25$ °C. The initial data of the metallo-supramolecular network (light grey symbols) have been vertically shifted by a factor 4/9.

III.2. Creep-Recovery Properties

In order to understand the influence of the metallo-supramolecular network on the deformation of the DDN, creep-recovery measurements were performed. This requires, first, to understand the response of the single networks (see Part A), before studying the creep-recovery properties of the DDN (see Part B).

A. Creep-Recovery Response of the Single Networks

A first creep-recovery test was performed at 25 °C on the metallo-supramolecular network containing 0.5 eq. of Zn²⁺ ions. As shown in Figure 11, a stress of 10 Pa is applied during 1800 s, followed by a recovery period between 1800 s and 3600 s. In the creep regime, the sample is continuously deformed, similarly to a viscoelastic liquid, despite the presence of the metal-ligand complexes. At this temperature and low stress applied, it is expected that the supramolecular junctions can break and reform, allowing the sample to slowly deform. Indeed, the LVE data of the network showed a solid-to-liquid transition at relatively short time (see Figure 2c). Then, when the stress is removed, little to no recovery is observed. At first glance, this could be attributed to the liquid-like behavior of the sample, which has lost its elastic memory of its initial configuration. However, if the latter is heated, its shape recovery takes place, at a rate that depends on the temperature (see the third time interval, t>3600s, in Figure 11).

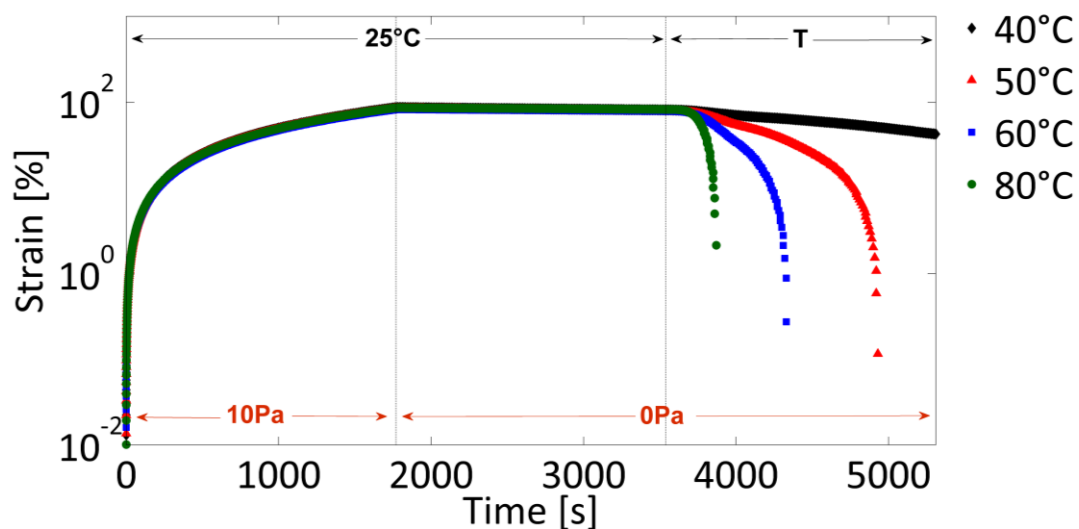


Figure 11: Creep-recovery curves (relative strain) for the metallo-supramolecular network with 0.5 eq. of Zn²⁺. The applied stress at time t=0 is 10 Pa at 25 °C. The recovery starts at 1800 s. Temperature is first fixed at 25 °C (from 1800 s to 3600 s) and is then increased to temperature T.

This is the author's peer reviewed, accepted manuscript. However, the online version of record will be different from this version once it has been copyedited and typeset.
PLEASE CITE THIS ARTICLE AS DOI: 10.1122/1.5000047

From this result, two main conclusions can be made. First, we can conclude that after its deformation under constant stress, the sample still contains some of its initial reversible bonds, which act as "permanent" crosslinkers. While their fraction is probably low, the proportion of these bonds is large enough to ensure keeping a percolated network, which elastically deforms when a stress is applied and goes back to its initial, equilibrium, shape once the stress is removed. Based on the results discussed in Section III.1, these few bonds with slower dynamics could correspond to chain entanglements. The latter can indeed only relax if the whole chain is able to diffuse, and are therefore characterized by a much longer lifetime compared to the lifetime of a single sticker. Second, this shape recovery process is taking place at the rhythm of the dissociation/association of the supramolecular bonds, which is speeded up when the temperature is increased. Indeed, the supramolecular bonds have to dissociate in order to allow the oriented percolated network to recover its initial configuration. A similar behavior has been observed previously in literature, as for example in the work of Matsumiya and Watanabe⁴² who studied the properties of multiblock copolymers of (Styrene-*b*-Isoprene-*b*-Styrene)_p (where $p = 1, 2, 3, \text{ or } 5$) in *n*-tetradecane, a selective solvent of the isoprene block. These systems display an elastic recovery even after deformations larger than the deformation corresponding to the complete extension of the full chain. The authors concluded that several copolymer chains can be involved in a strand of the remaining percolated network, connected together via only two associated blocks, and playing thus the role of chain extender. In Figure 11, we also see that the sample is able to creep at 25 °C. However, at this temperature, the dynamics of the supramolecular junctions is too slow to observe the sample recovery within the experimental time window. This can be explained if we consider that in the linear regime, a sticker will associate and dissociate several times with the same sticker before finding a new partner. Under a constant stress, one can imagine that this process is speeded up, leading to the reduction of the effective (rheological) lifetime of the bonds.^{52, 53}

Based on the above result, the creep-recovery of the different single metallo-supramolecular networks deformed under different stresses was then investigated. Temperature was fixed to 25 °C for the creep test, and followed by a recovery test during which the temperature was varied. First, the recovery temperature was kept at 25 °C for 30 min, then it was increased to 40 °C for 30 min, before being fixed to higher temperatures by steps of 20 °C every 30 min. The stress applied was fixed to 10 Pa, 100 Pa, 500 Pa and 1000 Pa. Results are summarized in Figure 12.

This is the author's peer reviewed, accepted manuscript. However, the online version of record will be different from this version once it has been copyedited and typeset.
PLEASE CITE THIS ARTICLE AS DOI: 10.1122/1.5000047

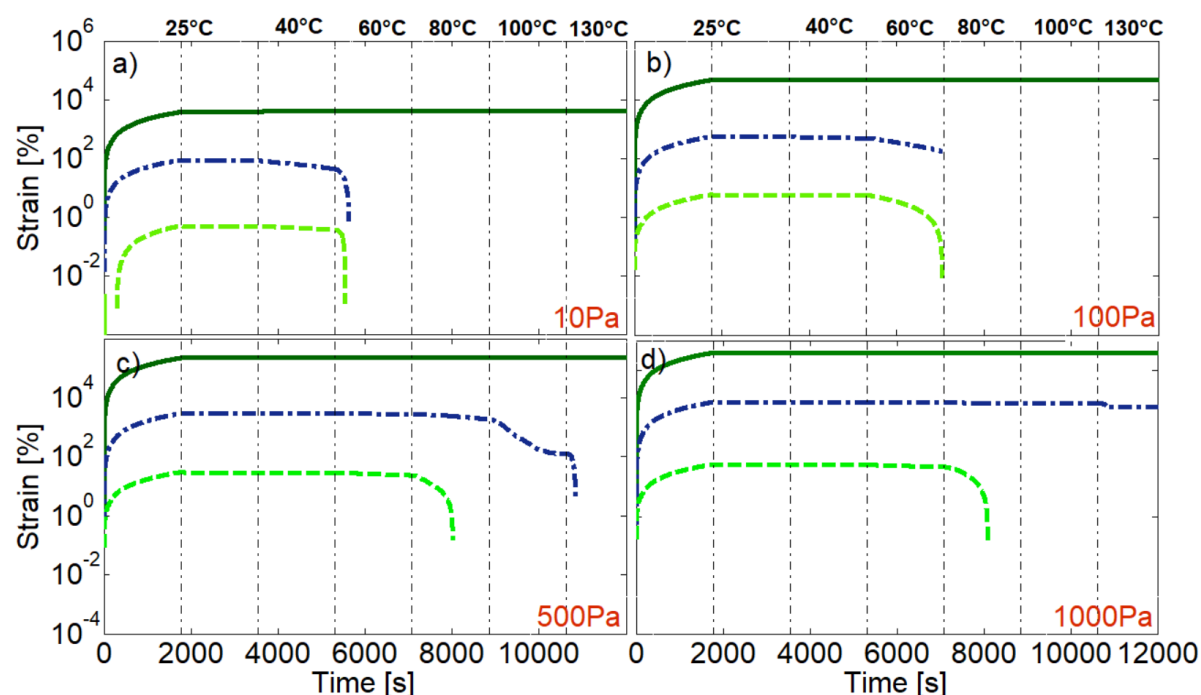


Figure 12: Creep-recovery curves (relative strain) for the PnBA27k-7Tpy reference sample (dark green, continuous curve) and the corresponding metallo-supramolecular networks with 0.5 eq. (dark blue, dashed-dotted curve) or 0.75 eq. (green, dashed curve) of Zn^{2+} . The applied stress is 10 Pa (a), 100 Pa (b), 500 Pa (c) or 1000 Pa (d). Creep temperature is 25 °C, while the recovery temperature is first fixed at 25 °C (from 1800s to 3600s), then at 40 °C and then increased by steps of 20 °C every 30 min.

When a constant stress is applied, the sample containing a larger amount of ions has a lower level of creep. This is consistent with the results obtained in the linear regime, where the relaxation time of the sticky chains was found to be governed by the lifetime of the supramolecular junctions, the latter being itself strongly dependent on the amount of ions (see Figure 4d). It should be noted that up to a stress of 500 Pa, the compliances related to these creep data superimpose, suggesting that the deformation stays in the linear regime. Only with a stress of 1000 Pa, the compliance is found to be slightly larger, entering the nonlinear regime of deformation (see SI, Figure S12).

Looking at the recovery properties, we see that the reference sample is not able to recover its initial shape whatever the temperature applied, i.e., this sample has no memory of its initial position and behaves as a liquid. This can be understood by its very poorly entangled state and its fast relaxation time (see Figure 3a). Furthermore, the more ions are present, the faster is the recovery of the network. At first glance, this result contradicts the idea according to which the sample recovery takes place at the rhythm of the association/dissociation of the stickers, since in this case, sample PnBA27k-7Tpy-0.5eq should recover faster than sample PnBA27k-7Tpy-0.75eq. However, this apparent discrepancy

This is the author's peer reviewed, accepted manuscript. However, the online version of record will be different from this version once it has been copyedited and typeset.
PLEASE CITE THIS ARTICLE AS DOI: 10.1122/1.5000473

can be understood based on the network connectivity, which is the dominant factor in these experiments. Indeed, the larger density of associated stickers in sample *PnBA27k-7Tpy-0.75eq* increases its elastic modulus, which leads to a lower deformation reached at the end of the creep test (at $t=1800s$), compared to the deformation of sample *PnBA27k-7Tpy-0.5eq*. Consequently, the probability to damage the initial network is smaller with 0.75eq. of ions, which speeds up the sample recovery. Thus, for these systems, this limited deformation seems to govern the recovery response of the network. After applying a high, nonlinear, stress (1000 Pa), the network containing 0.5eq. of ions is unable to recover its initial shape. This suggests that the initial network is broken and does not contain a percolated path anymore. As already mentioned, the presence of a larger amount of ions allows keeping the network cohesion and limits the sample deformation, which explains why, under the same stress, the 0.75eq. Zn^{2+} network still deforms elastically.

The behavior of the single dynamic covalent network is rather different (Figure 13). If the same stress is applied, both the reference (uncrosslinked) sample *PnBA473K-18Ald* diluted at 30 wt% with the short *PnBA22k* matrix and the crosslinked network *PnBA473K-18Ald-0.5eq* diluted with the same *PnBA22k* display much less creep than the metallo-supramolecular network, despite their lower (or inexistent) density of crosslinks. This is attributed to the very long lifetime of the entanglements in the reference system (due to the high molar mass of the chains). This lifetime becomes even longer in the crosslinked system since part of these entanglements is trapped between two dynamic covalent bonds acting as nearly permanent junctions (see Figure 6). These entanglements limit the deformability of the systems. Contrary to the metallo-supramolecular networks, the DCN is able to partially recover its initial shape at 25 °C. This was expected since the dynamic covalent bonds are not broken and do not create new connections during the time the sample is deformed. Therefore, the sample recovery is not governed by the dynamic covalent bonds. However, after this fast partial recovery, slower recovery modes appear, which are speeded up with increasing temperature. At 25 °C, the influence of the short chain matrix, which governs the rate at which the local equilibration of the network takes place, is observed in Figure 6b. It is thus probable that the Constraint Release Rouse process of the DCN slows down the final stage of the network recovery, which requires the equilibration of longer chain segments. Finally, when a nonlinear stress of 1000 Pa is applied (see the corresponding compliance data in SI, fig S12), the DCN mostly recovers its initial configuration, however, a small residual deformation (0.5-1 %) persists at high temperature.

This is the author's peer reviewed, accepted manuscript. However, the online version of record will be different from this version once it has been copyedited and typeset.
PLEASE CITE THIS ARTICLE AS DOI: 10.1122/1.5000047

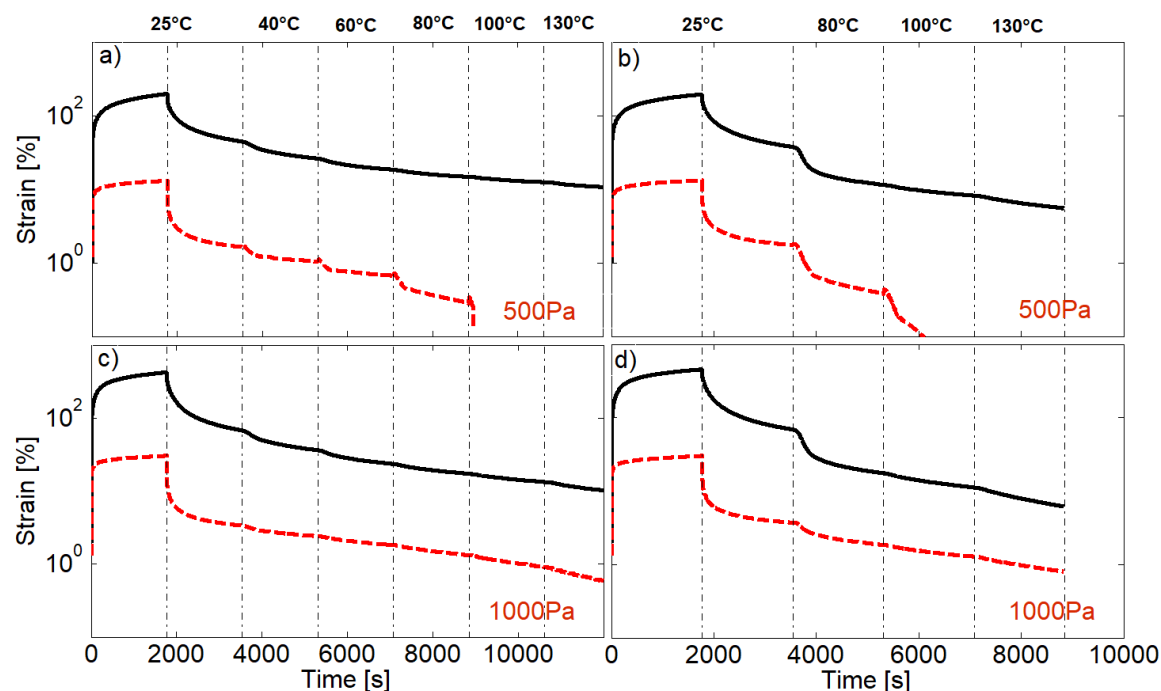


Figure 13: Creep-recovery curves (relative strain) for the PnBA473k-18Ald reference sample (black, continuous curve) and the corresponding dynamic covalent network PnBA473k-18Ald-0.5eq (red, dashed curve). Both samples are diluted to 30% in a PnBA22k. Creep temperature is 25 °C, while the recovery temperature is first fixed at 25 °C (from 1800s to 3600s), then at 40 °C (a and c) or 80 °C (b and d), and then increased by steps of 20 °C every 30 min.

B. Creep-recovery Response of the Double Dynamic Networks

Based on the creep-recovery behavior of the single DCN and metallo-supramolecular network individually, we can now investigate the properties of the DDN as a function of temperature and amount of metal ions added to the network. The experimental results are summarized in Figure 14.

We first observe that for a given applied stress, the creep of the DDN is less important than the creep observed in the single DCN. The presence of the metallo-supramolecular network reduces the elastic deformation of the DCN, which cannot take place faster than the dissociation/association dynamics of the junctions of the metallo-supramolecular network. Similarly, while the single metallo-supramolecular network significantly creeps when a stress is applied (see Figure 12), its deformability is largely reduced by the presence of the DCN. Indeed, as long as the junctions of the DCN behave as permanent crosslinks, the latter governs the sample extensibility. This synergistic effect on the sample deformation, where the weaker bonds play the role of sacrificial junctions and the stronger network ensures the network connectivity, has been already observed previously with other double dynamic networks.⁵³ In particular, a few studies have proposed to use creep-recovery tests to analyze the creep

This is the author's peer reviewed, accepted manuscript. However, the online version of record will be different from this version once it has been copyedited and typeset.
PLEASE CITE THIS ARTICLE AS DOI: 10.1122/1.5000473

resistance of different vitrimers. If the latter are characterized by a fast exchange dynamics of their covalent bonds, they are susceptible to creep. Some strategies have been tried to overcome this effect, which include integrating a limited number of permanent static crosslinks,⁵⁴ or using stronger dynamic covalent bonds such as alkoxyamine based dynamic covalent bonds.²³ Another strategy consists in using two types of dynamic covalent bonds^{19, 24} in a double dynamic network to improve the mechanical properties. However, this leads to little control over the creep-recovery properties without changing the entire system. Recently, it was shown that dual networks obtained by adding metal-ligand junctions in a vitrimer containing imine groups also allows to reduce the creep as the addition of the metal-ligand junctions increases the cross-linking density of the network. The creep reduction was found to be more important with stronger metal-ligand complexes.²⁵ In our material, we rather use interpenetrated networks to combine the dissipative properties of metal-ligand complexes with the elasticity of the vitrimer systems, as this allows a larger tunability of the double dynamic network. Indeed, in this case, the local equilibration of the loosely crosslinked DCN is not only dependent on the lifetime of the metallo-supramolecular junctions, but also on the time the entire sticky chains need to diffuse to relax and release entanglements between the two networks, which can be tuned by modifying the topology of the sticky chains, as well as the lifetime and number of stickers per chain.²⁰

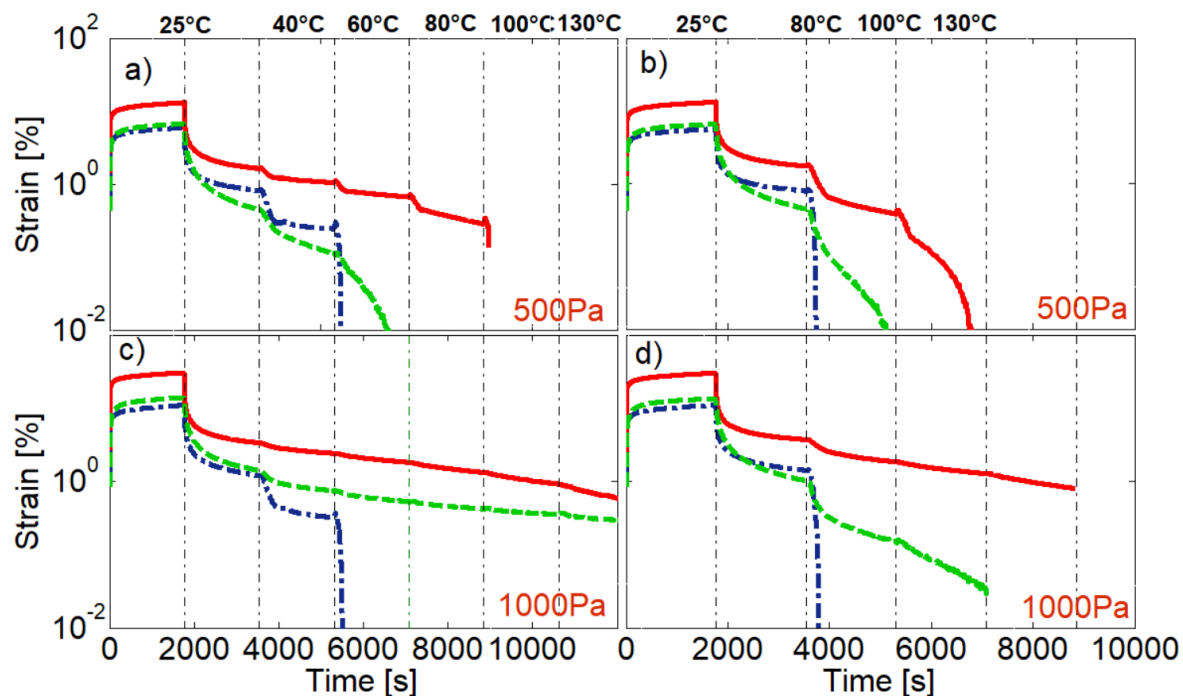


Figure 14: Creep-recovery curves of the DCN single network (red continuous curve) and of the double dynamic networks with 0.5eq. (blue, dashed-dotted curve) and 0.75eq. (green, dashed curve) of Zn^{2+} . The applied stress is 500Pa (a and b) and 1000Pa (c and d) at 25 °C. Creep temperature is 25 °C, while

This is the author's peer reviewed, accepted manuscript. However, the online version of record will be different from this version once it has been copyedited and typeset.
PLEASE CITE THIS ARTICLE AS DOI: 10.1122/1.5000047

the recovery temperature is first fixed at 25 °C (from 1800s to 3600s) and is then increased by steps of 20 °C from 40 °C (a and c) or 80 °C (b and d).

The DDN is able to fully recover its initial configuration, even under a stress of 1000 Pa (Figure 14, the residual strain < 1%). Since the amplitude of the strain reached at 500Pa and 1000Pa is limited by the presence of the metallo-supramolecular network, the local deformation for the DDN is not as large as in the single DCN, and the memory of the network is therefore preserved. This creep-recovery behavior also largely differs from the one observed for the single metallo-supramolecular networks. In particular, with 0.5eq. Zn²⁺, the single network showed larger creep under a stress of 1000Pa, leading to nearly no recovery (see Figure 12).

Just after the creep regime, the DDNs are all able to recover a part of their initial shapes at 25 °C, similarly as the single DCN. If a larger amount of ions is added, this first recovery process is more pronounced. Then, the sample recovery can be speeded up by heating the samples. Similarly to the effect of decreasing the temperature on the recovery behavior of the single metallo-supramolecular networks (see Figure 11), slowing down the dynamics of the supramolecular bonds by the addition of a larger amount of ions leads to a slower recovery process. As illustrated in Figure 15, this confirms that the dynamics of the weaker networks controls the equilibration and recovery properties of the stable network. The latter are thus largely dependent on the lifetime and density of the fast (metallo-supramolecular) stickers, on temperature and on the importance of the stress or deformation applied, giving large room to tune the properties of the DDN.

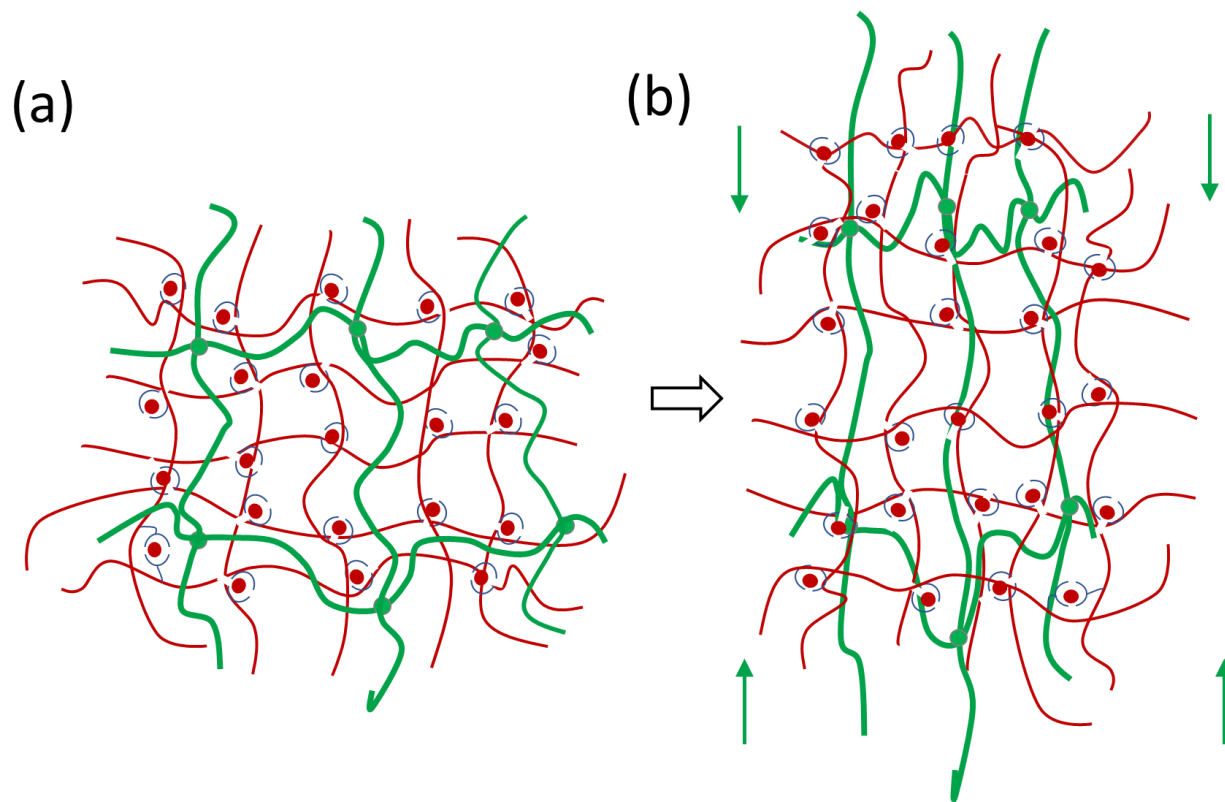


Figure 15: Illustration of the recovery process. (a) Before the creep test, both the dynamic covalent network (in green) and the metallo-supramolecular network (in red) are at equilibrium. (b) At the end of the creep test, the DCN (the bonds of which are static at 25 °C) is stretched while the metallo-supramolecular network is equilibrated since its supramolecular junctions are constantly dissociating and associating again. The recovery of the DCN can only take place at the rhythm of the dissociation/association dynamics of the metallo-supramolecular junctions.

IV. Conclusion

Through controlled synthesis, we were able to create well-defined double dynamic polymer networks based on side-functionalized PnBA chains. One of these networks is highly crosslinked by metal-ligand junctions characterized by a fast association/dissociation dynamics, while the other network is sparsely crosslinked with slow dynamic covalent bonds. The properties of the corresponding single networks and of the double dynamic networks were investigated through linear shear rheology and creep-recovery testing.

First, linear rheological data have shown that the viscoelastic response of the single metallo-supramolecular networks is controlled by the sticker lifetime, the temperature dependence of which is well described by an Arrhenius equation. At long times, the observed thermo-rheological behavior suggests the existence of a few topological constraints such as few inter-chain entanglements, which need longer time to relax, especially when a larger amount of metal ions is added. This small fraction

of slow-relaxing chains also gives to these metallo-supramolecular single networks good memory properties, and enhance their ability to recover their initial shape after a creep test.

Then, looking at the linear properties of the stable dynamic covalent network diluted either in a matrix of short *PnBA* chains or in a metallo-supramolecular network matrix, we have shown that the local equilibration of the DCN is taking place by a Constraint Release Rouse process, which is controlled by the motions of the supramolecular chains, themselves being controlled by the amount of ions and by the temperature. It is therefore possible to tune the rate at which the DCN can explore its surrounding. Based on creep-recovery experiments, we have shown the synergistic effect between the metallo-supramolecular network and the DCN, where the weaker bonds play the role of sacrificial junctions and the stronger network ensures the network connectivity. The sample recovery, which can take place upon heating is dependent on several parameters. First, it depends on the ability of the DDN to keep its network coherence or connectivity. The latter is enhanced if a denser metallo-supramolecular network is used, as it reduces the possible creep of the sample and increases its elastic memory. Second, the sample recovery also depends on the association-dissociation dynamics of the metallo-supramolecular bonds, as it fixes how fast the stretched DCN can come back to their equilibrium conformation and can recover their initial shape after a large deformation has been applied. Adjusting the dynamics of the weak network is thus a key process to govern the viscoelastic response of the slow network.

Supplementary Material

The supplementary material contains information about the synthesis and the preparation protocol of the different systems, about the rheological behavior of DDN containing different weight fractions of DCN, and about the creep compliance data of metallo-supramolecular systems.

Acknowledgments

This work was funded by the EU (Horizon 2020, Marie Skłodowska-Curie ITN DoDyNet, Grant Agreement No. 765811) and by the French Community of Belgium through ARC project no 16/21-076 (A.A., C.-A.F. and E.V.R.). E.V.R. is Research Associate of the FRS-FNRS.

1. Liu, J., Tan, C. S. Y., Yu, Z., Li, N., Abell, C., and Scherman, O. A., "Tough Supramolecular Polymer Networks with Extreme Stretchability and Fast Room-Temperature Self-Healing," *Advanced Materials* 29, 1605325 (2017).
2. Fan, J., Huang, J., Gong, Z., Cao, L., and Chen, Y., "Toward Robust, Tough, Self-Healable Supramolecular Elastomers for Potential Application in Flexible Substrates," *ACS Applied Materials & Interfaces* 13, 1135-1144 (2021).

This is the author's peer reviewed, accepted manuscript. However, the online version of record will be different from this version once it has been copyedited and typeset.
PLEASE CITE THIS ARTICLE AS DOI: 10.1122/1.5111111

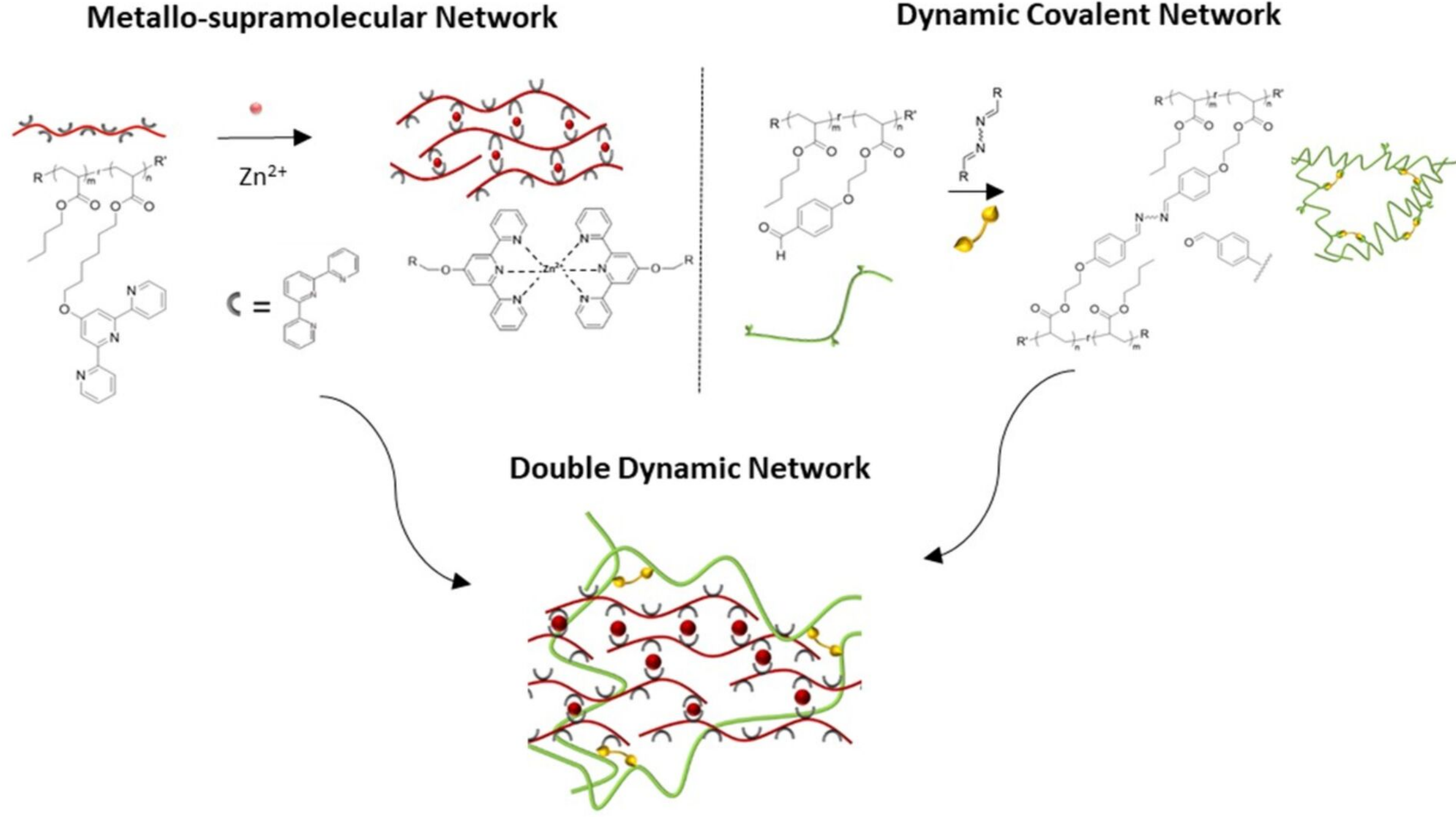
3. Kim, C., Nakagawa, S., Seshimo, M., Ejima, H., Houjou, H., and Yoshie, N., "Tough Supramolecular Elastomer via Entropy-Driven Hydrogen Bonds between Vicinal Diols," *Macromolecules* 53, 4121-4125 (2020).
4. Appel, E. A., Loh, X. J., Jones, S. T., Biedermann, F., Dreiss, C. A., and Scherman, O. A., "Ultrahigh-Water-Content Supramolecular Hydrogels Exhibiting Multistimuli Responsiveness," *Journal of the American Chemical Society* 134, 11767-11773 (2012).
5. Guo, M., Pitet, L. M., Wyss, H. M., Vos, M., Dankers, P. Y. W., and Meijer, E. W., "Tough Stimuli-Responsive Supramolecular Hydrogels with Hydrogen-Bonding Network Junctions," *Journal of the American Chemical Society* 136, 6969-6977 (2014).
6. Wang, Y. J., Zhang, X. N., Song, Y., Zhao, Y., Chen, L., Su, F., Li, L., Wu, Z. L., and Zheng, Q., "Ultrastiff and Tough Supramolecular Hydrogels with a Dense and Robust Hydrogen Bond Network," *Chemistry of Materials* 31, 1430-1440 (2019).
7. Creton, C., "50th Anniversary Perspective: Networks and Gels: Soft but Dynamic and Tough," *Macromolecules* 50, 8297-8316 (2017).
8. Chen, Q., Chen, H., Zhu, L., and Zheng, J., "Fundamentals of double network hydrogels," *Journal of Materials Chemistry B* 3, 3654-3676 (2015).
9. Zhao, X., Chen, X., Yuk, H., Lin, S., Liu, X., and Parada, G., "Soft Materials by Design: Unconventional Polymer Networks Give Extreme Properties," *Chemical Reviews* 121, 4309-4372 (2021).
10. Gong, J. P., Katsuyama, Y., Kurokawa, T., and Osada, Y., "Double-Network Hydrogels with Extremely High Mechanical Strength," *Adv. Mater* 15, 1155-1158 (2003).
11. Nakajima, T., Ozaki, Y., Namba, R., Ota, K., Maida, Y., Matsuda, T., Kurokawa, T., and Gong, J. P., "Tough Double-Network Gels and Elastomers from the Nonprestretched First Network," *ACS Macro Letters* 8, 1407-1412 (2019).
12. Jeong-Yun, S., Zhao, X., Illeperuma, W. R. K., Chaudhuri, O., Oh, K. H., Mooney, D. J., Vlassak, J. J., and Suo, Z., "Highly stretchable and tough hydrogels," *Nature* 489, 133-136 (2012).
13. Ducrot, E., Chen, Y., Bulters, M., Sijbesma, R. P., and Creton, C., "Toughening Elastomers with Sacrificial Bonds and Watching Them Break," *Science* 344, 186-189 (2014).
14. Wu, J., Cai, L.-H., and Weitz, D. A., "Tough Self-Healing Elastomers by Molecular Enforced Integration of Covalent and Reversible Networks," *Adv. Mater*, 1702616 (2017).
15. Jiang, C., Mai, Y., Li, W., and Liao, B., "Supersoft, Stretchable, Tough, and Adhesive Elastomers with Dual Metal-Ionic Crosslinked Double-Network Structure," *Macromolecular Chemistry and Physics* 221, 1900516 (2020).
16. Foster, E. M., Lensmeyer, E. E., Zhang, B., Chakma, P., Flum, J. A., Via, J. J., Sparks, J. L., and Konkolewicz, D., "Effect of Polymer Network Architecture, Enhancing Soft Materials Using Orthogonal Dynamic Bonds in an Interpenetrating Network," *ACS Macro Lett.*, 495-499 (2017).
17. Peng, W. L., You, Y., Xie, P., Rong, M. Z., and Zhang, M. Q., "Adaptable Interlocking Macromolecular Networks with Homogeneous Architecture Made from Immiscible Single Networks," *Macromolecules*, 584-593 (2020).
18. Roy, N., Buhler, E., and Lehn, J.-M., "Double dynamic self-healing polymers: supramolecular and covalent dynamic polymers based on the bis-iminocarbohydrazide motif," *Polym Int*, 1400-1405 (2014).
19. Neal, J. A., Mozhdzhi, D., and Guan, Z., "Enhancing Mechanical Performance of a Covalent Self-Healing Material by Sacrificial Noncovalent Bonds," *J. Am. Chem. Soc.* 137, 4846-4850 (2015).
20. Yang, H., Ghiassinejad, S., van Ruymbeke, E., and Fustin, C.-A., "Tunable Interpenetrating Polymer Network Hydrogels Based on Dynamic Covalent Bonds and Metal-Ligand Bonds," *Macromolecules* 53, 6956-6967 (2020).
21. Wang, Y., Liang, D., Suo, Z., and Jia, K., "Synergy of noncovalent interlink and covalent toughener for tough hydrogel adhesion," *Extreme Mechanics Letters* 39, 100797 (2020).
22. Yu, Z., Zhang, Y., Gao, Z. J., Ren, X. Y., and Gao, G. H., "Enhancing mechanical strength of hydrogels via IPN structure," *Journal of Applied Polymer Science* 134, 44503 (2016).

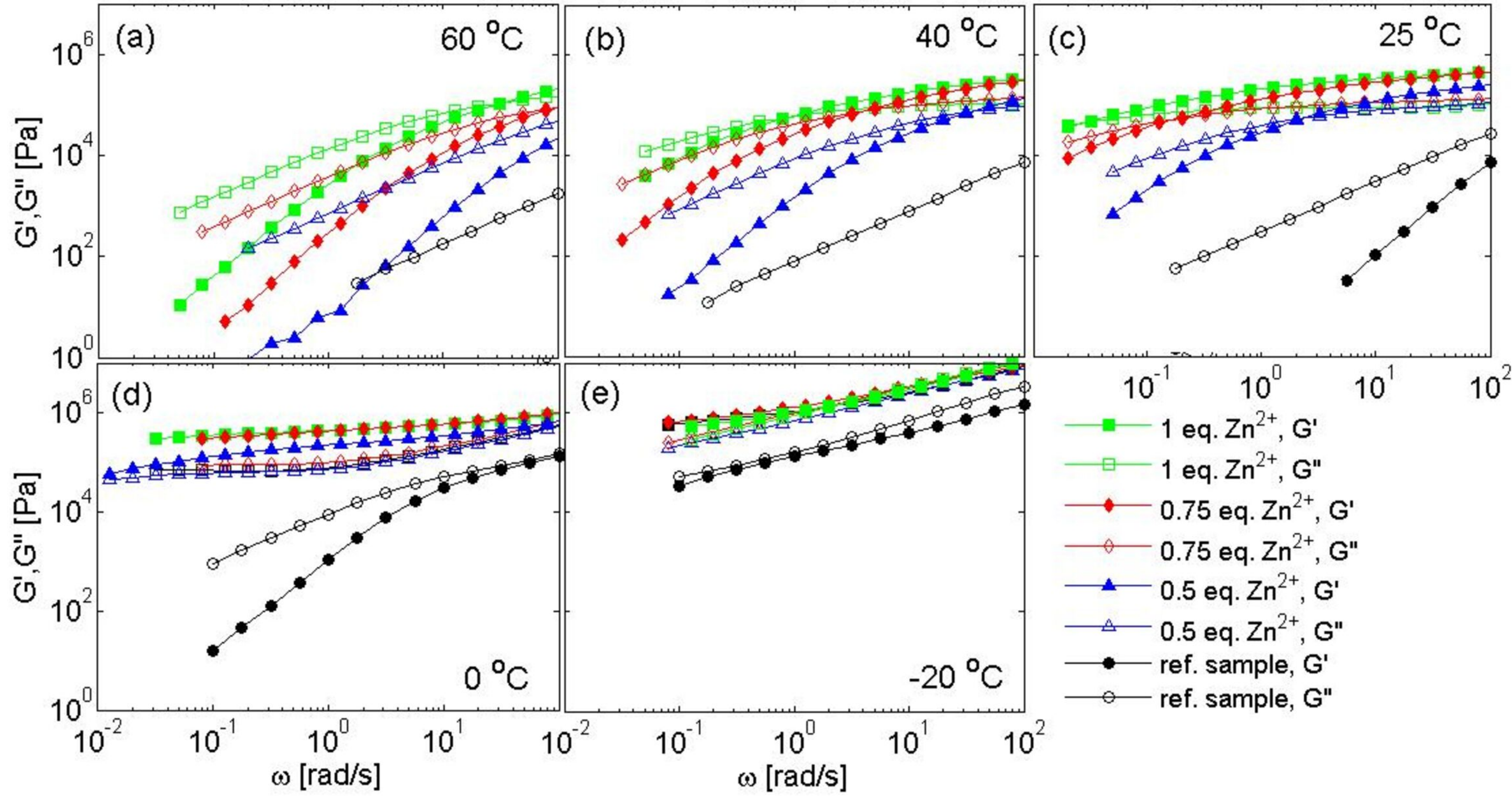
23. Li, L., Chen, X., Jin, K., Bin Rusayyis, M., and Torkelson, J. M., "Arresting Elevated-Temperature Creep and Achieving Full CrossLink Density Recovery in Reprocessable Polymer Networks and Network Composites via Nitroxide-Mediated Dynamic Chemistry," *Macromolecules*, 1452-1464 (2021).
24. Liu, Y., Tang, Z., Wu, S., and Guo, B., "Integrating Sacrificial Bonds into Dynamic Covalent Networks toward Mechanically Robust and Malleable Elastomers," *ACS Macro Letters* 8, 193-199 (2019).
25. Wang, S., Ma, S., Li, Q., Xu, X., Wang, B., Huang, K., Liu, Y., and Zhu, J., "Facile Preparation of Polyimine Vitrimers with Enhanced Creep Resistance and Thermal and Mechanical Properties via Metal Coordination," *Macromolecules* 53, 2919-2931 (2020).
26. Mayumi, K., Marcellan, A., Ducouret, G., Creton, C., and Narita, T., "Stress-Strain Relationship of Highly Stretchable Dual Cross-Link Gels: Separability of Strain and Time Effect," *ACS Macro Letters* 2, 1065-1068 (2013).
27. Narita, T., Mayumi, K., Ducouret, G., and Hébraud, P., "Viscoelastic Properties of Poly(vinyl alcohol) Hydrogels Having Permanent and Transient Cross-Links Studied by Microrheology, Classical Rheometry, and Dynamic Light Scattering," *Macromolecules* 46, 4174-4183 (2013).
28. Li, C.-H., Wang, C., Keplinger, C., Zuo, J.-L., Jin, L., Sun, Y., Zheng, P., Cao, Y., Lissel, F., Linder, C., You, X.-Z., and Bao, Z., "A highly stretchable autonomous self-healing elastomer," *Nature Chemistry* 8, 618-624 (2016).
29. Van Zee, N. J., and Nicolaÿ, R., "Vitrimers: Permanently crosslinked polymers with dynamic network topology," *Progress in Polymer Science* 104, 101233 (2020).
30. Hammer, L., Van Zee, N. J., and Nicolaÿ, R., "Dually Crosslinked Polymer Networks Incorporating Dynamic Covalent Bonds," *Polymers* 13 (2021).
31. Zhuge, F., Brassinne, J., Fustin, C.-A., van Ruymbeke, E., and Gohy, J.-F., "Synthesis and Rheology of Bulk Metallo-Supramolecular Polymers from Telechelic Entangled Precursors," *Macromolecules* 50, 5165-5175 (2017).
32. Zhuge, F., Hawke, L. G. D., Fustin, C.-A., Gohy, J.-F., and van Ruymbeke, E., "Decoding the linear viscoelastic properties of model telechelic metallo-supramolecular polymers," *Journal of Rheology*, 1245 (2017).
33. Van Ruymbeke, E., "Preface: Special Issue on Associating Polymers," *Journal of Rheology* 61, 1099-1102 (2017).
34. Leibler, L., Rubinstein, M., and Colby, R. H., "Dynamics of Reversible Networks," *Macromolecules*, 4701-4707 (1991).
35. Chen, Q., Tudryn, G. J., and Colby, R. H., "Ionmer dynamics and the sticky Rouse model," *Journal of Rheology* 57, 1441-1462 (2013).
36. Ferry, J. D., *Viscoelastic Properties of Polymers, 3rd Edition* (Wiley, New York, 1980).
37. Munstedt, H., "Rheological experiments at constant stress as efficient method to characterize polymer materials," *Journal of Rheology* 58, 565 (2014).
38. Hawke, L. G. D., Ahmadi, M., Goldansaz, H., and van Ruymbeke, E., "Viscoelastic properties of linear associating poly(n-butyl acrylate) chains," *Journal of Rheology* 60, 297-310 (2016).
39. Li, Y., Pyromali, C., Zhuge, F., Fustin, C.-A., Gohy, J.-F., Vlassopoulos, D., and van Ruymbeke, E., "Dynamics of entangled metallo-supramolecular polymer networks combining stickers with different lifetimes," *Journal of Rheology* (2022).
40. Ruymbeke, E. v., Muliawan, E. B., Vlassopoulos, D., Gao, H., and Matyjaszewski, K., "Melt rheology of star polymers with large number of small arms, prepared by crosslinking poly(n-butyl acrylate) macromonomers via ATRP," *European Polymer Journal* 47, 746-751 (2011).
41. Likhtman, A. E., and McLeish, T. C. B., "Quantitative Theory for Linear Dynamics of Linear Entangled Polymers," *Macromolecules* 35, 6332-6343 (2002).
42. Schwarzl, F. R., "Numerical calculation of storage and loss modulus from stress relaxation data for linear viscoelastic materials," *Rheologica Acta* 10, 165-173 (1971).
43. Gonçalves, M. A. D., Dias, R. C. S., and Costa, M. R. P. F. N., "Prediction and Experimental Characterization of the Molecular Architecture of FRP and ATRP Synthesized Polyacrylate Networks," *Macromolecular Symposia* 289, 1-17 (2010).

This is the author's peer reviewed, accepted manuscript. However, the online version of record will be different from this version once it has been copyedited and typeset.
PLEASE CITE THIS ARTICLE AS DOI: 10.1122/1.511111

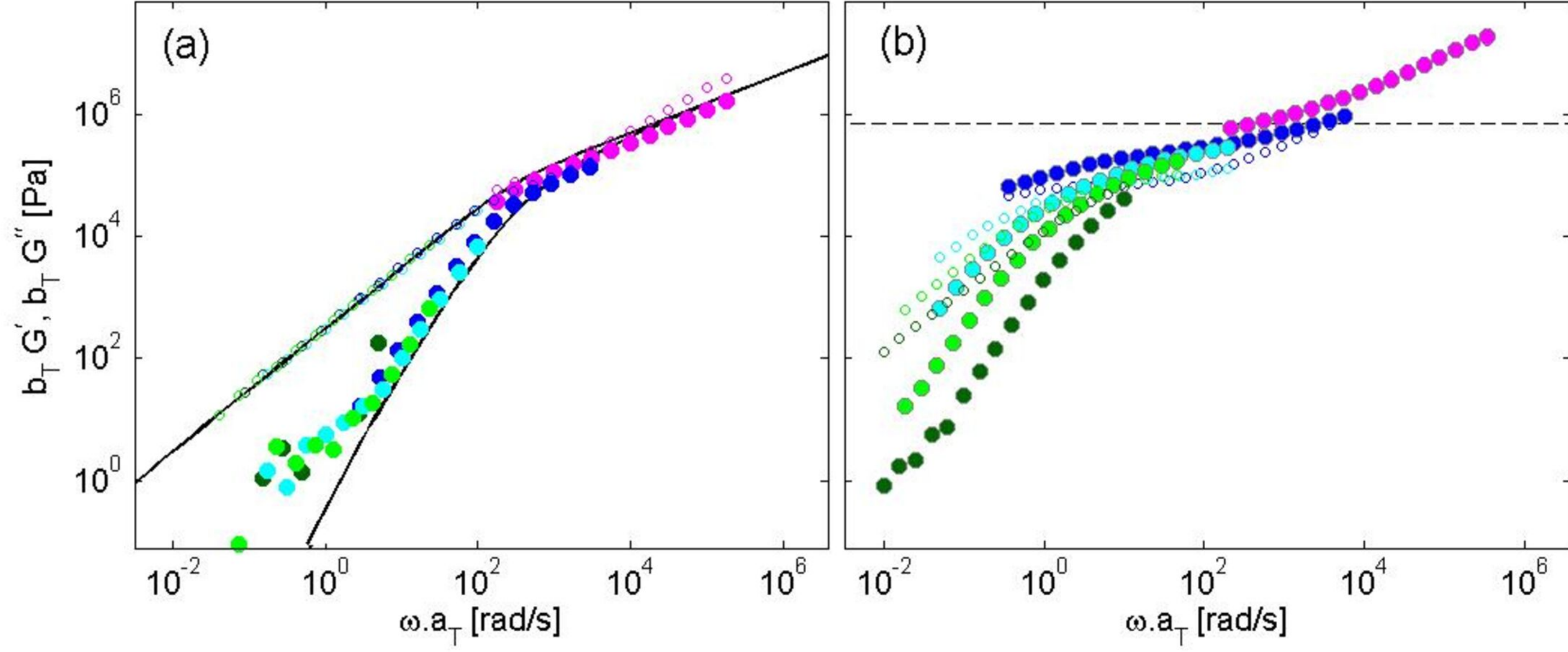
44. Chen, H., Zhang, J., Yu, W., Cao, Y., Cao, Z., and Tan, Y., "Control Viscoelasticity of Polymer Networks with Crosslinks of Superposed Fast and Slow Dynamics," *Angewandte Chemie International Edition* 60, 22332-22338 (2021).
45. Wu, S., and Chen, Q., "Advances and New Opportunities in the Rheology of Physically and Chemically Reversible Polymers," *Macromolecules* 55, 697-714 (2022).
46. Verjans, J., André, A., Van Ruymbeke, E., and Hoogenboom, R., "Physically Cross-Linked Polybutadiene by Quadruple Hydrogen Bonding through Side-Chain Incorporation of Ureidopyrimidinone with Branched Alkyl Side Chains," *Macromolecules* 55, 928-941 (2022).
47. Ahmadi, M., and Seiffert, S., "Dynamic Model Metallo-Supramolecular Dual-Network Hydrogels with Independently Tunable Network Crosslinks," *Journal of Polymer Science* 58, 330-342 (2020).
48. Holyer, R. H., Hubbard, C. D., Kettle, S. F. A., and Wilkins, R. G., "The Kinetics of Replacement Reactions of Complexes of the Transition Metals with 2,2',2''-Terpyridine," *Inorganic Chemistry* 5, 622-625 (1966).
49. Calì, R., Rizzarelli, E., Sammartano, S., and Siracusa, G., "Thermodynamics of 2,2',2''-terpyridinecopper(II) complexes in aqueous solution," *Transition Metal Chemistry* 4, 328-332 (1979).
50. van Ruymbeke, E., Shchetnikava, V., Matsumiya, Y., and Watanabe, H., "Dynamic Dilution Effect in Binary Blends of Linear Polymers with Well-Separated Molecular Weights," *Macromolecules* 47, 7653-7665 (2014).
51. Watanabe, H., "Viscoelasticity and dynamics of entangled polymers," *Progress in Polymer Science* 24, 1253-1403 (1999).
52. Evans, E., "Probing the Relation Between Force—Lifetime—and Chemistry in Single Molecular Bonds," *Annual Review of Biophysics and Biomolecular Structure* 30, 105-128 (2001).
53. Amin, D., and Wang, Z., "Nonlinear rheology and dynamics of supramolecular polymer networks formed by associative telechelic chains under shear and extensional flows," *Journal of Rheology* 64, 581-600 (2020).
54. Li, L., Chen, X., Jin, K., and Torkelson, J. M., "Vitrimers Designed Both To Strongly Suppress Creep and to Recover Original Cross-Link Density after Reprocessing: Quantitative Theory and Experiments," *Macromolecules*, 5537-5546 (2018).

This is the author's peer reviewed, accepted manuscript. However, the online version of record will be different from this version once it has been copyedited and typeset.
PLEASE CITE THIS ARTICLE AS DOI: 10.1122/8.0000473

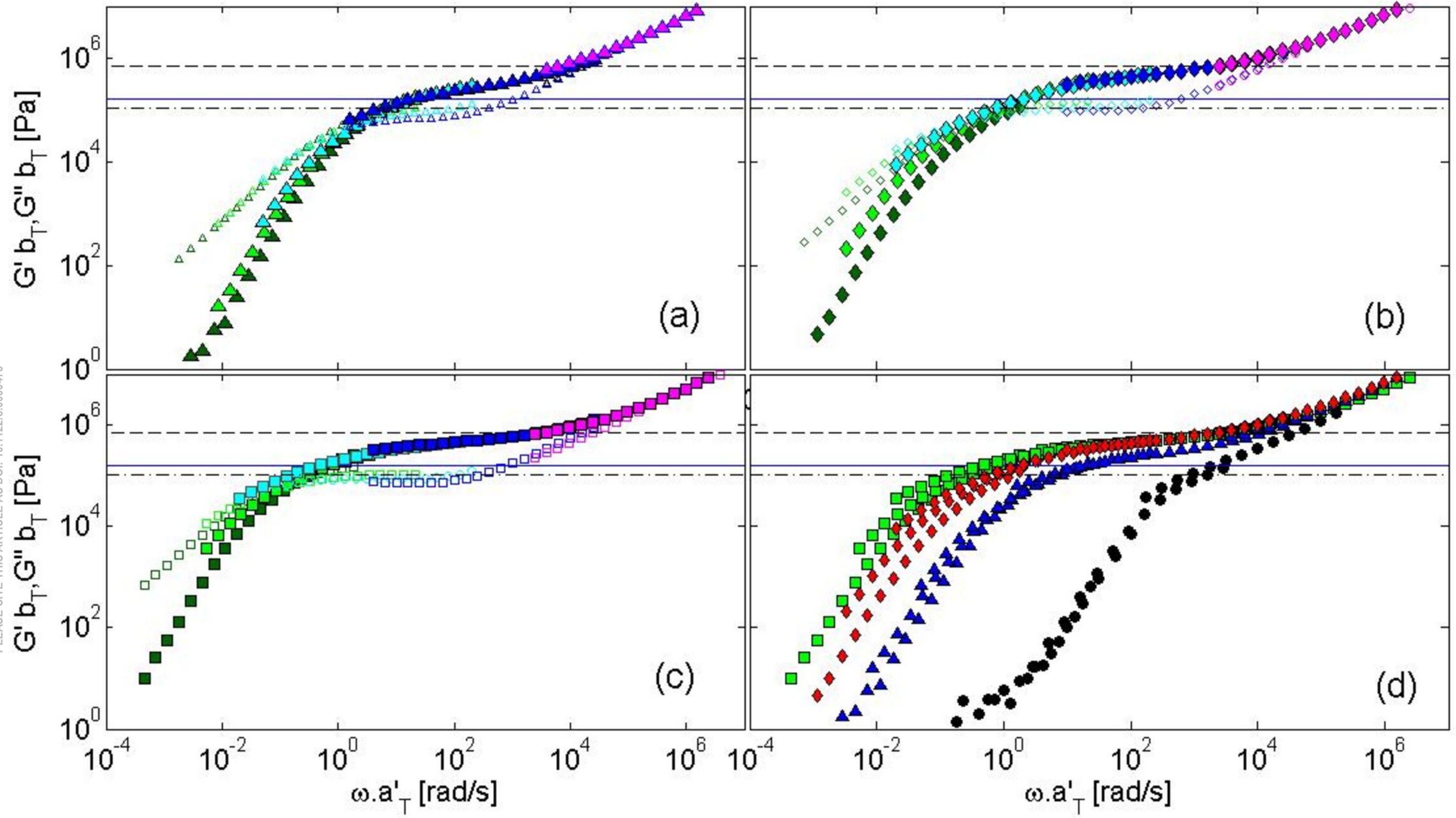




This is the author's peer reviewed, accepted manuscript. However, the online version of record will be different from this version once it has been copyedited and typeset.
PLEASE CITE THIS ARTICLE AS DOI: 10.1122/1.5000473



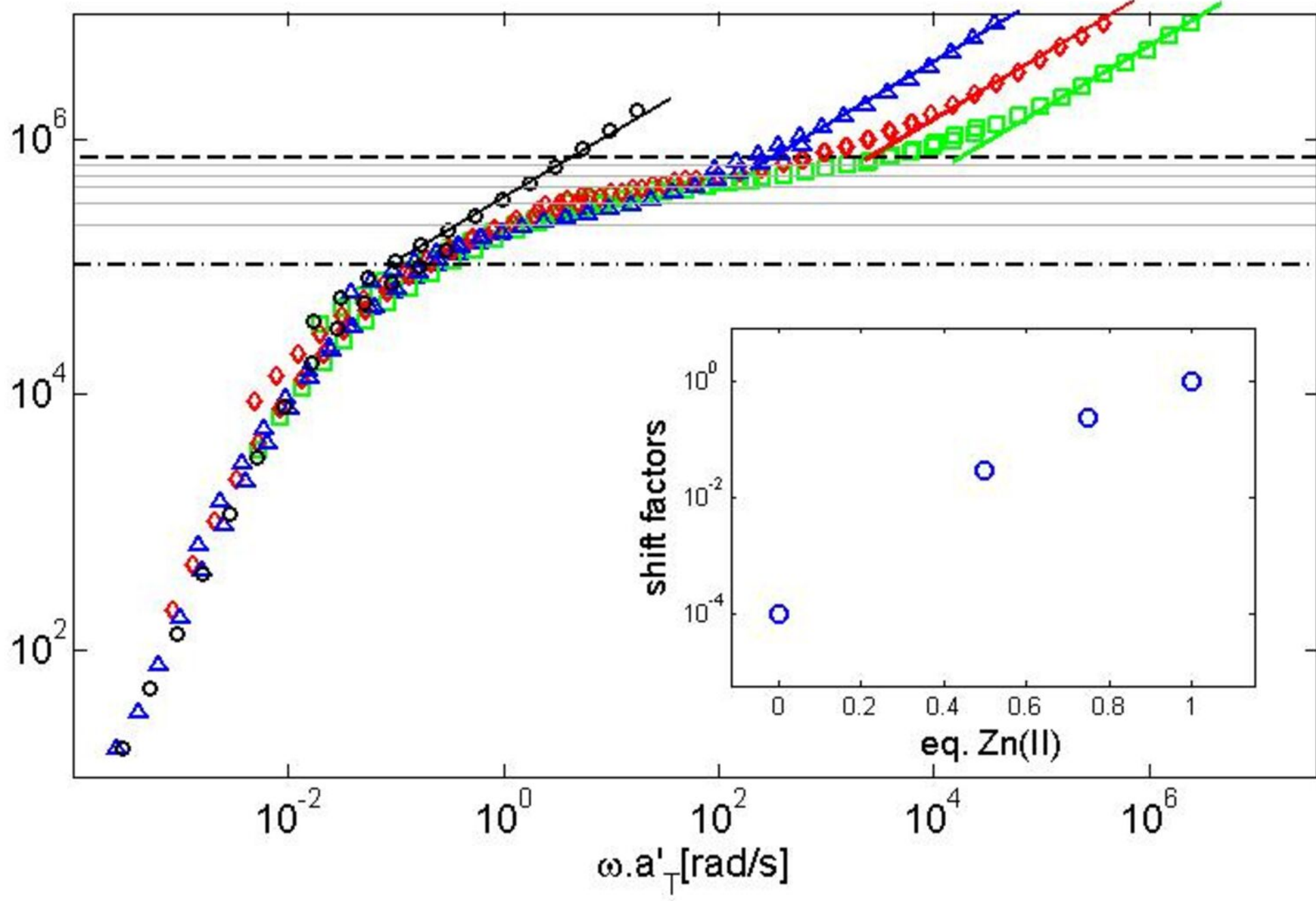
This is the author's peer reviewed, accepted manuscript. However, the online version of record will be different from this version once it has been copyedited and typeset.
PLEASE CITE THIS ARTICLE AS DOI: 10.1122/1.8.0000473



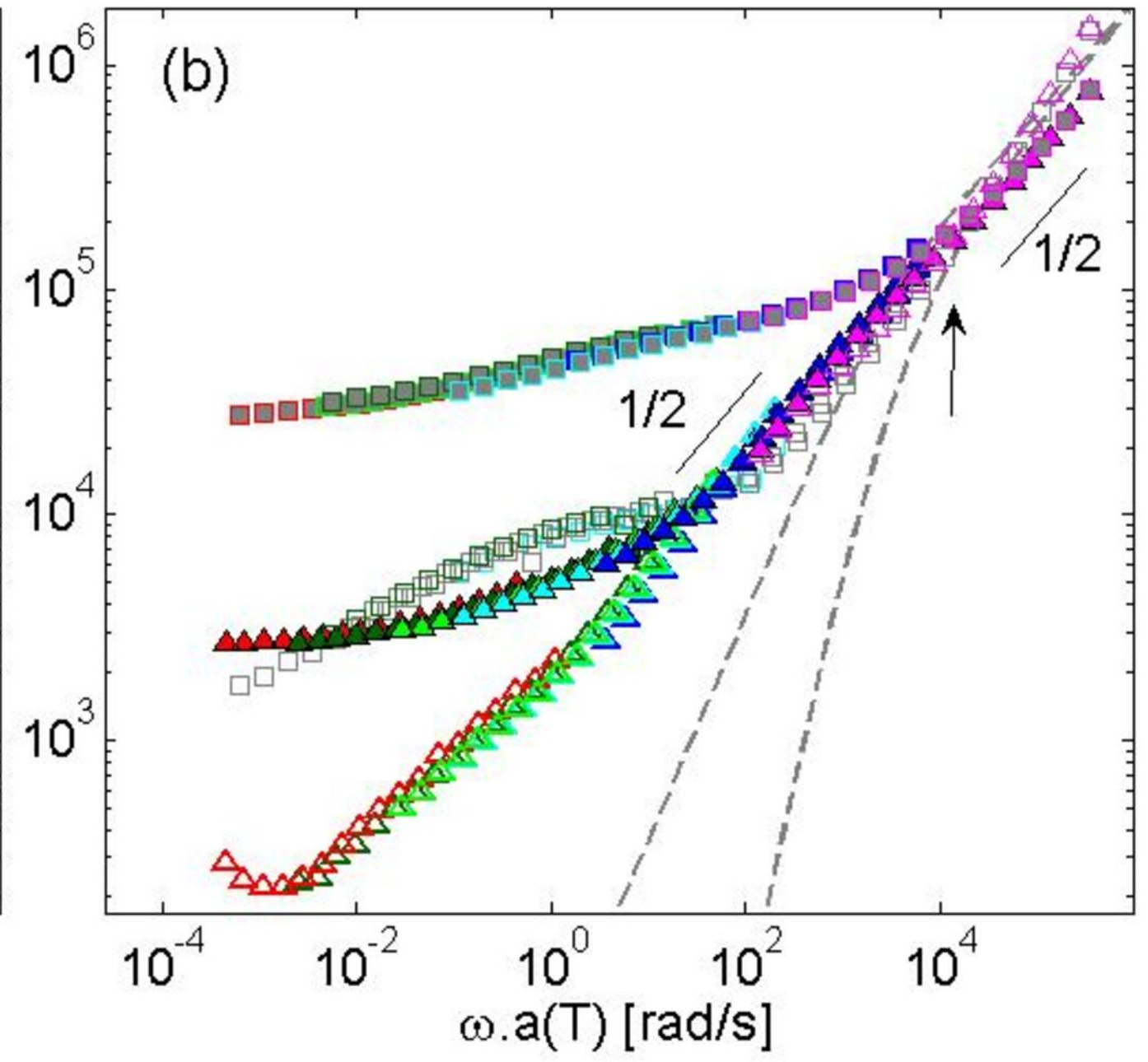
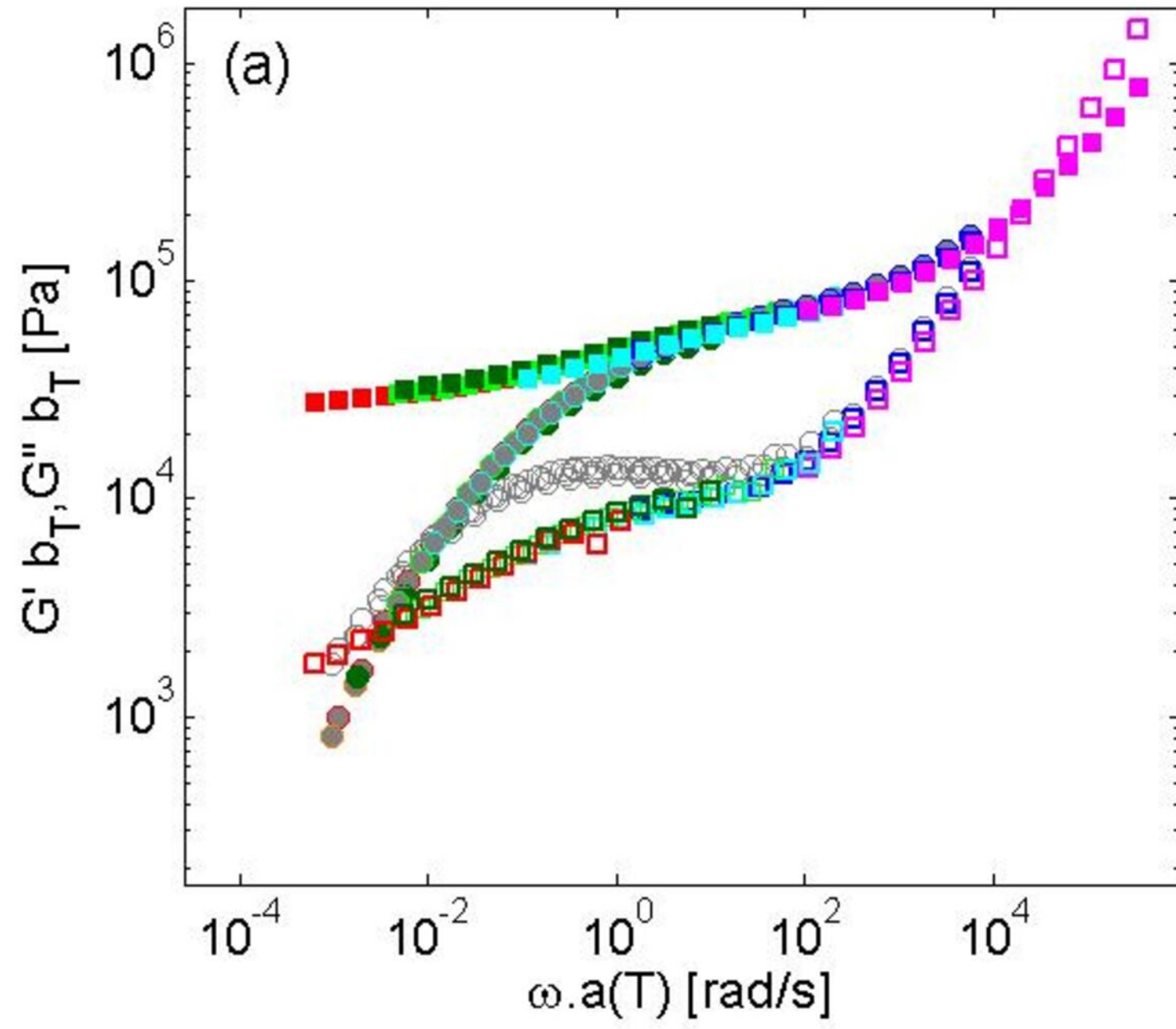
This is the author's peer reviewed, accepted manuscript. However, the online version of record will be different from this version once it has been copyedited and typeset.

PLEASE CITE THIS ARTICLE AS DOI: 10.1122/8.0000473

$G' b_T$ [Pa]

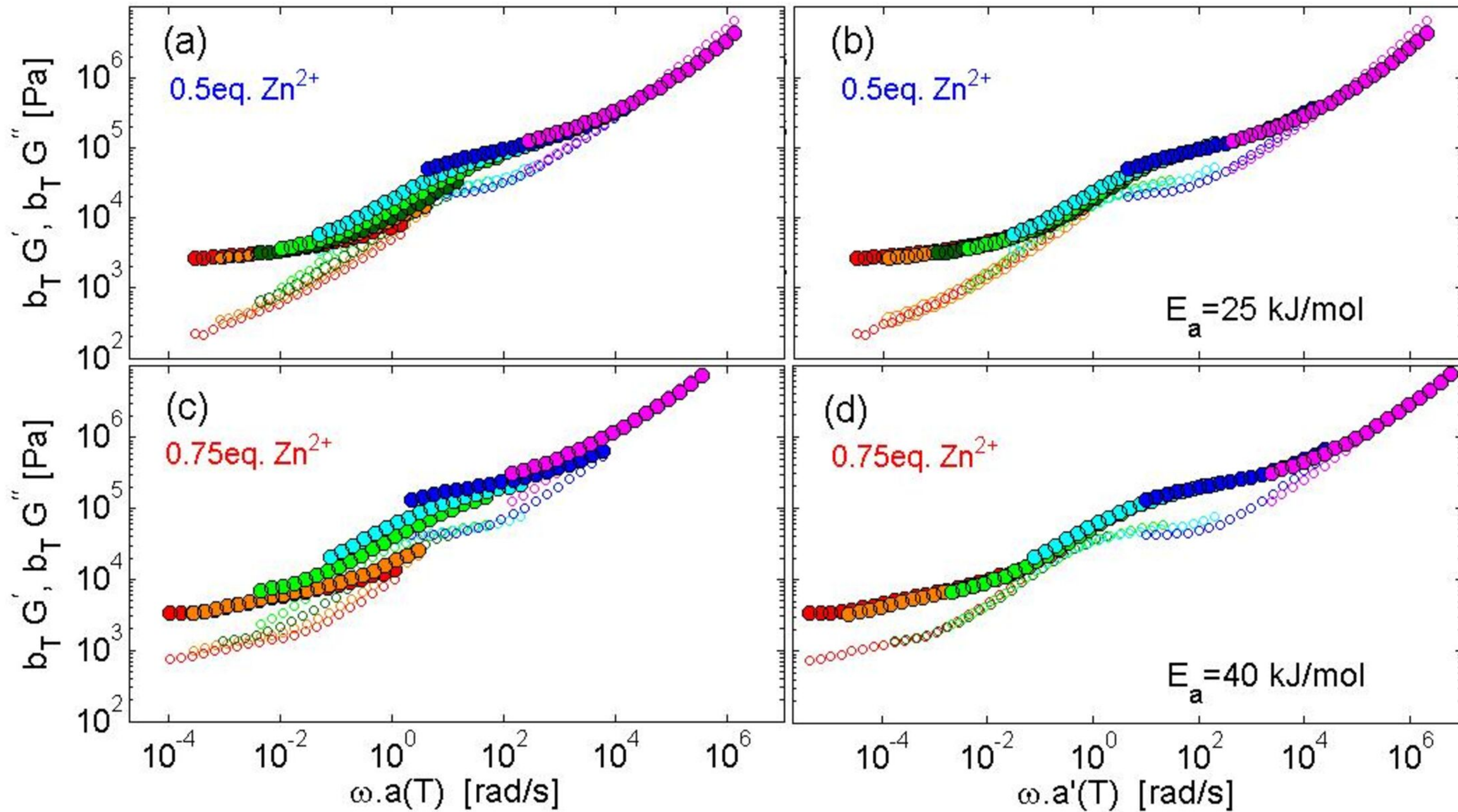


This is the author's peer reviewed, accepted manuscript. However, the online version of record will be different from this version once it has been copyedited and typeset.
 PLEASE CITE THIS ARTICLE AS DOI: 10.1122/1.5000473

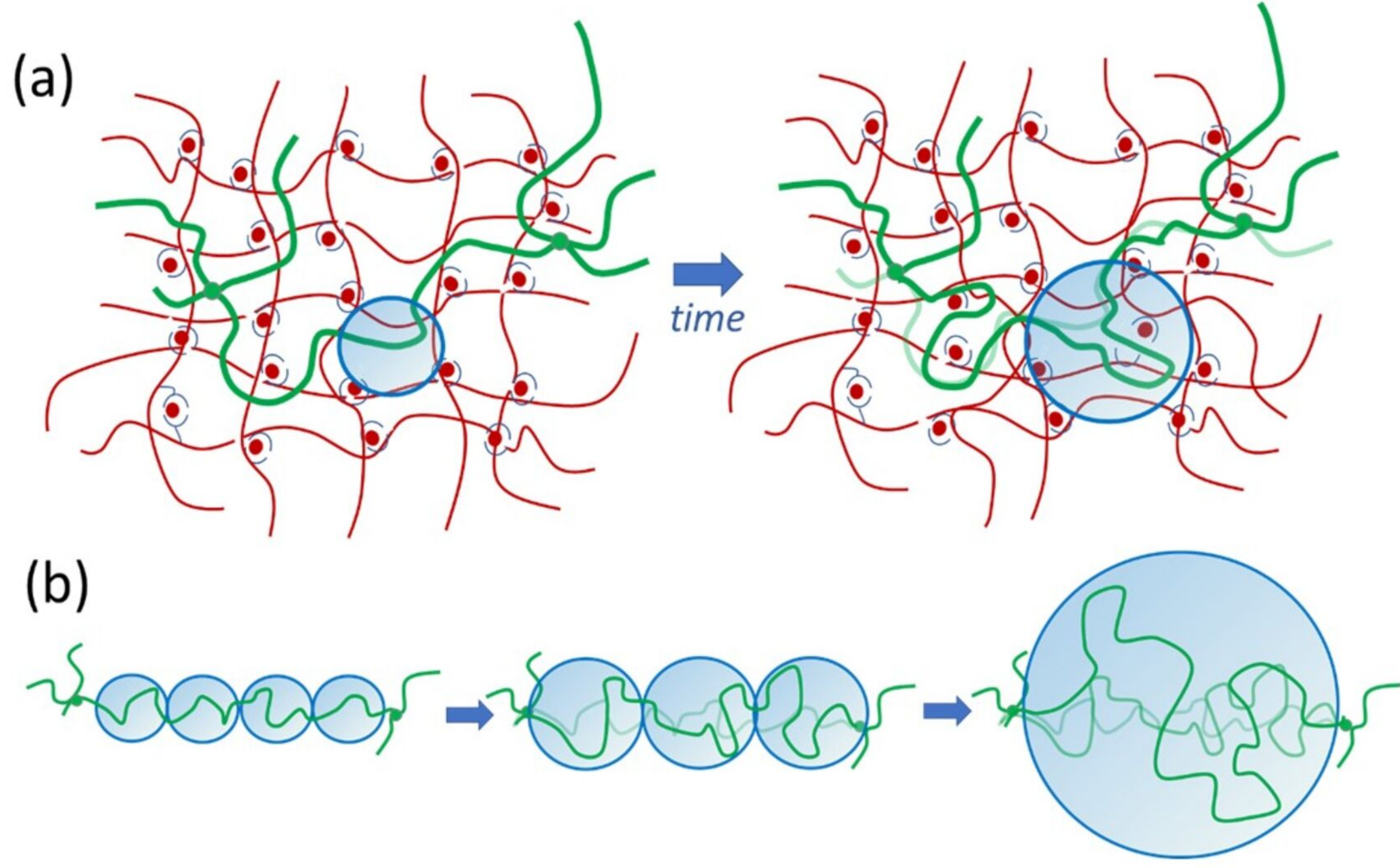




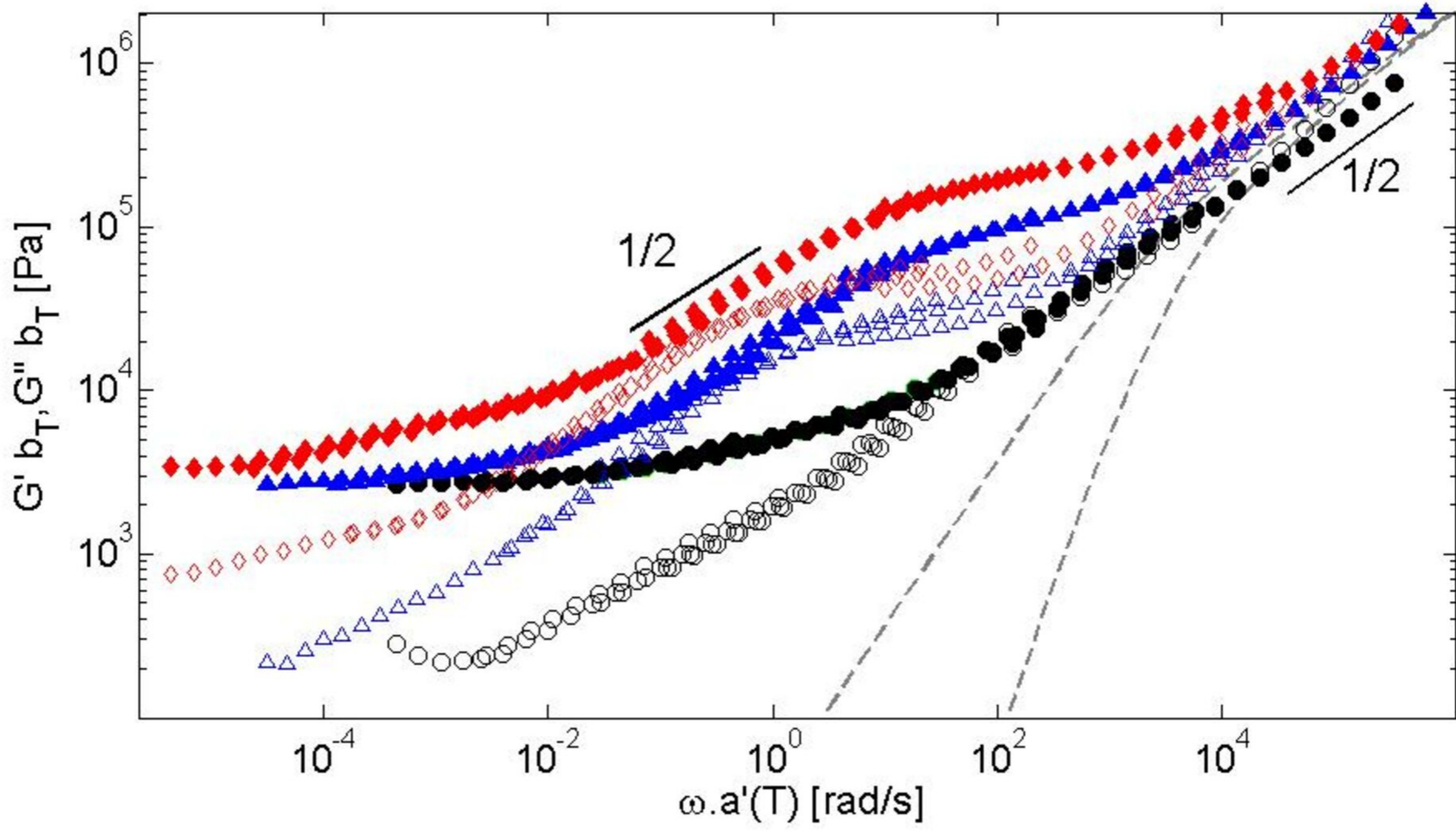
This is the author's peer reviewed, accepted manuscript. However, the online version of record will be different from this version once it has been copyedited and typeset.
PLEASE CITE THIS ARTICLE AS DOI: 10.1122/1.5000473



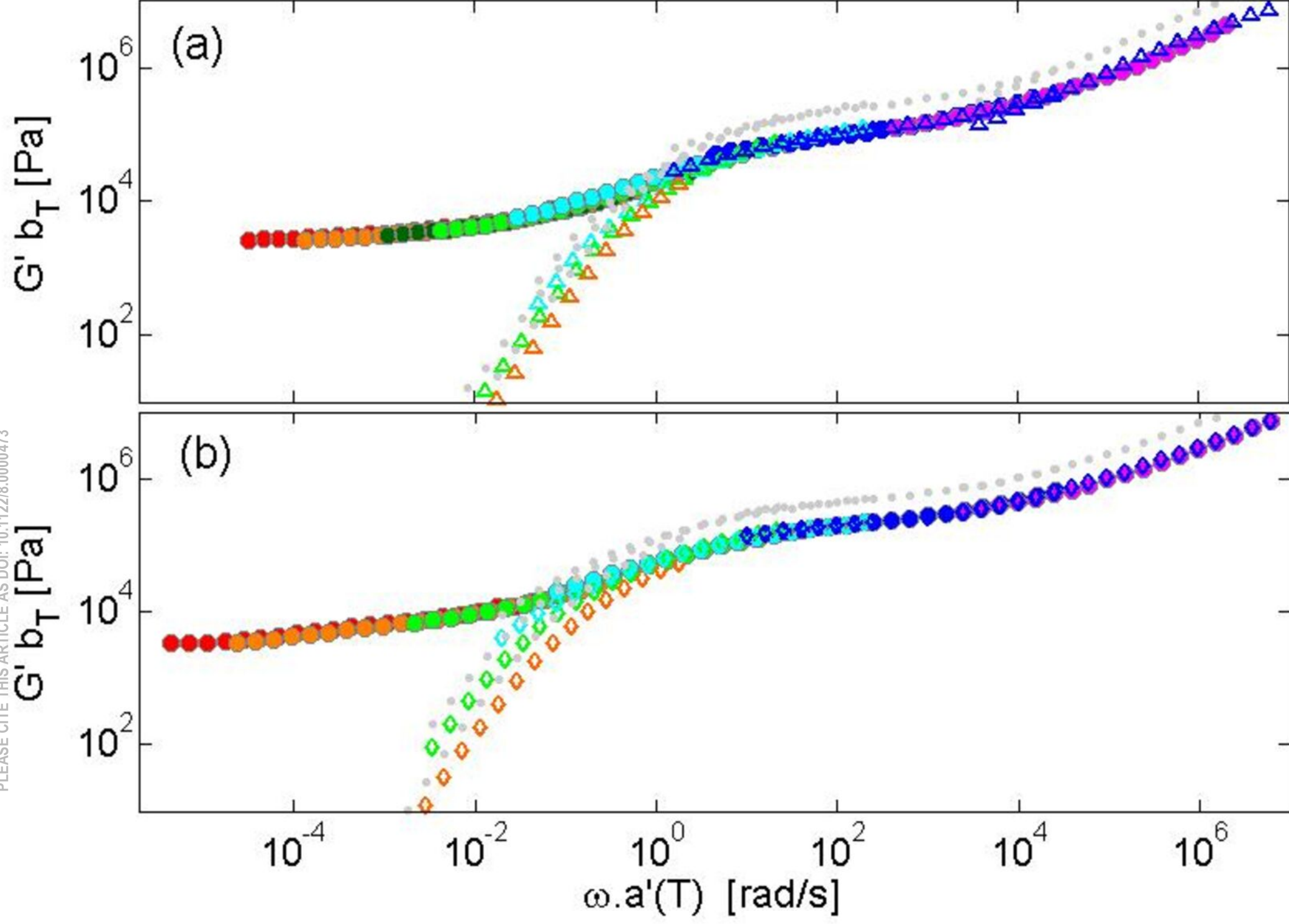
This is the author's peer reviewed, accepted manuscript. However, the online version of record will be different from this version once it has been copyedited and typeset.
PLEASE CITE THIS ARTICLE AS DOI: 10.1122/8.0000473



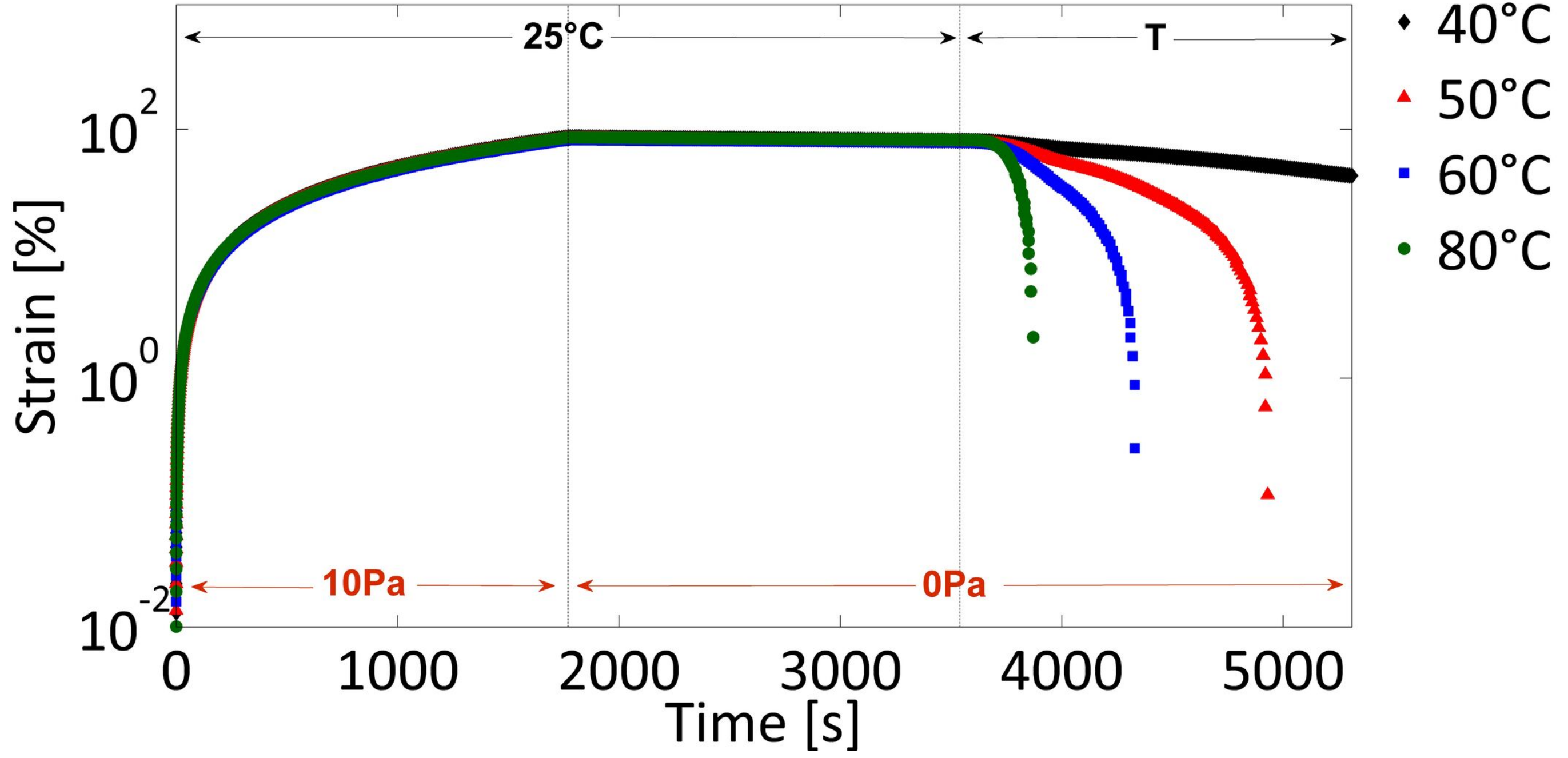
This is the author's peer reviewed, accepted manuscript. However, the online version of record will be different from this version once it has been copyedited and typeset.
PLEASE CITE THIS ARTICLE AS DOI: 10.1122/8.0000473



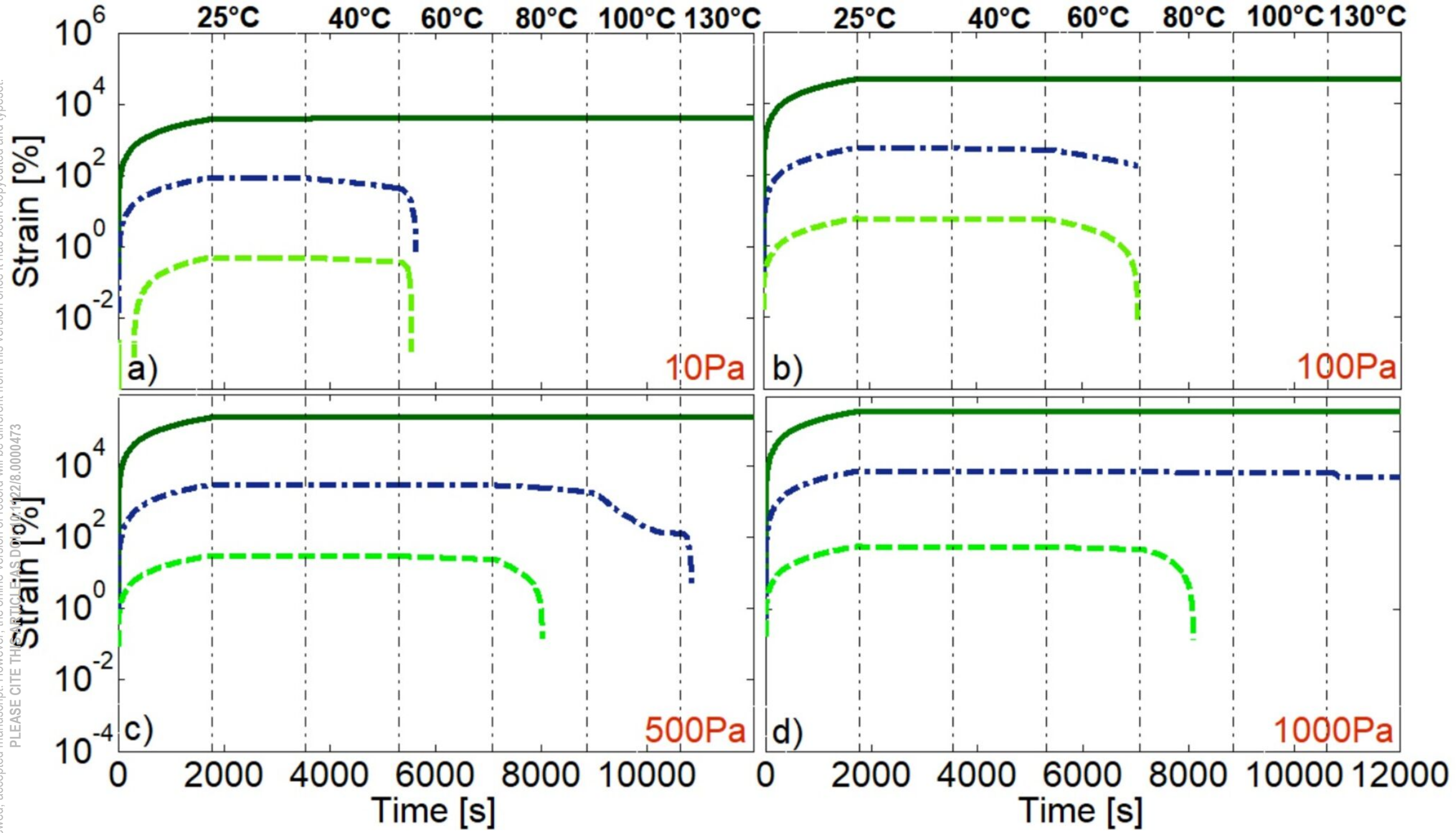
This is the author's peer reviewed, accepted manuscript. However, the online version of record will be different from this version once it has been copyedited and typeset.
PLEASE CITE THIS ARTICLE AS DOI: 10.1122/8.0000473



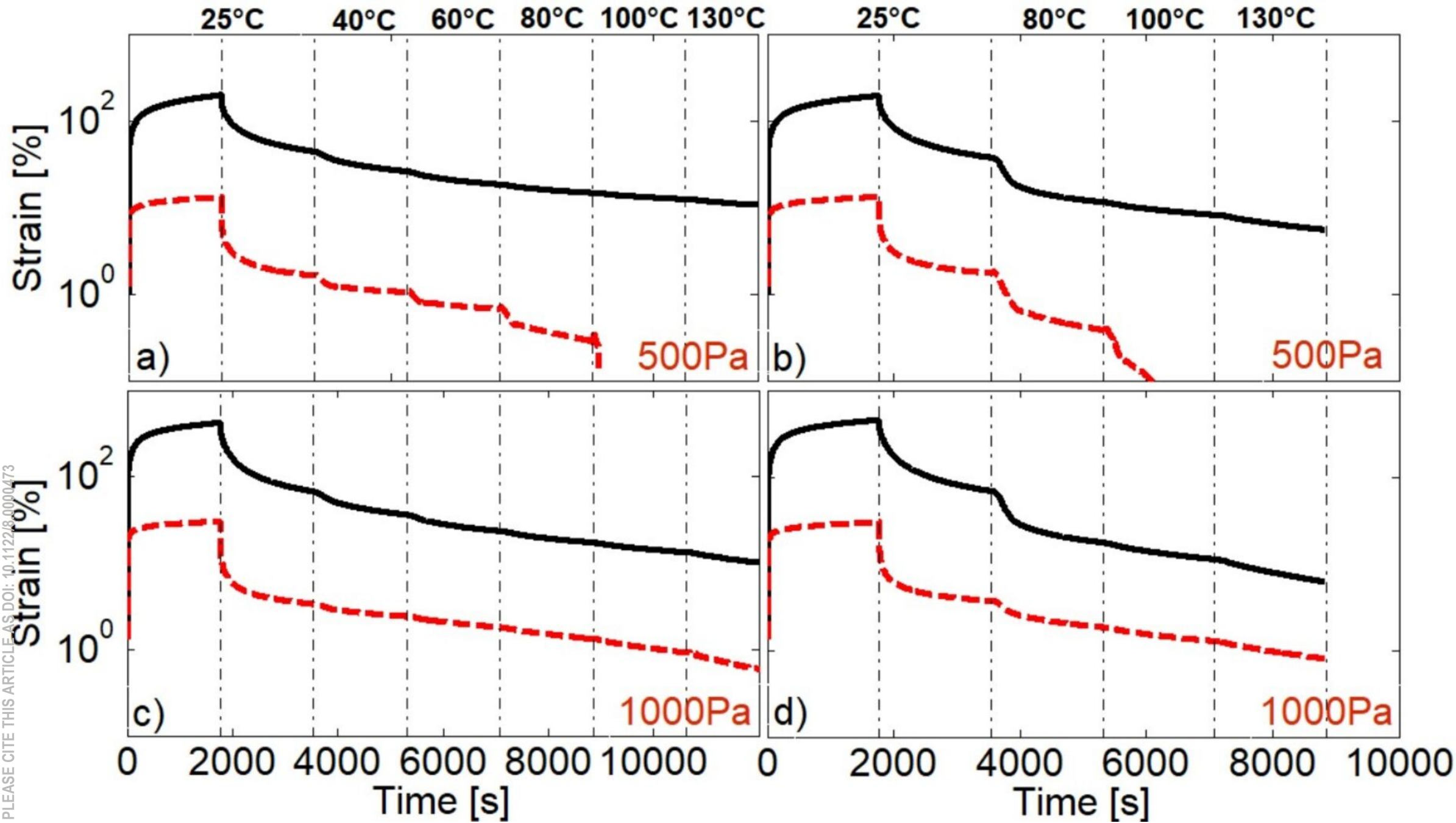
This is the author's peer reviewed, accepted manuscript. However, the online version of record will be different from this version once it has been copyedited and typeset.
PLEASE CITE THIS ARTICLE AS DOI: 10.1122/1.5000473



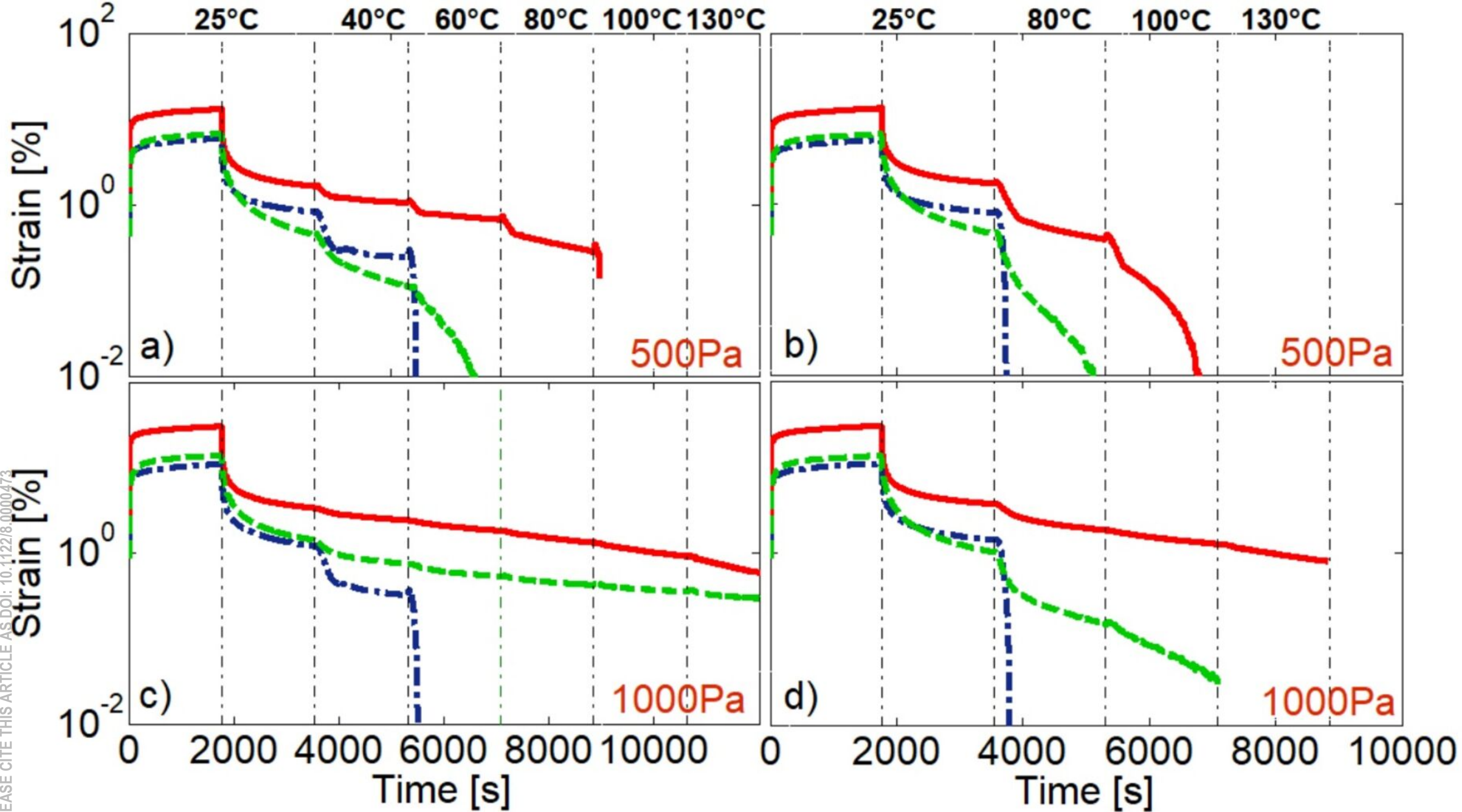
This is the author's peer reviewed, accepted manuscript. However, the online version of record will be different from this version once it has been copyedited and typeset.
PLEASE CITE THIS ARTICLE AS DOI: 10.1122/1.528.0000473



This is the author's peer reviewed, accepted manuscript. However, the online version of record will be different from this version once it has been copyedited and typeset.
PLEASE CITE THIS ARTICLE AS DOI: 10.1122/1.5000473

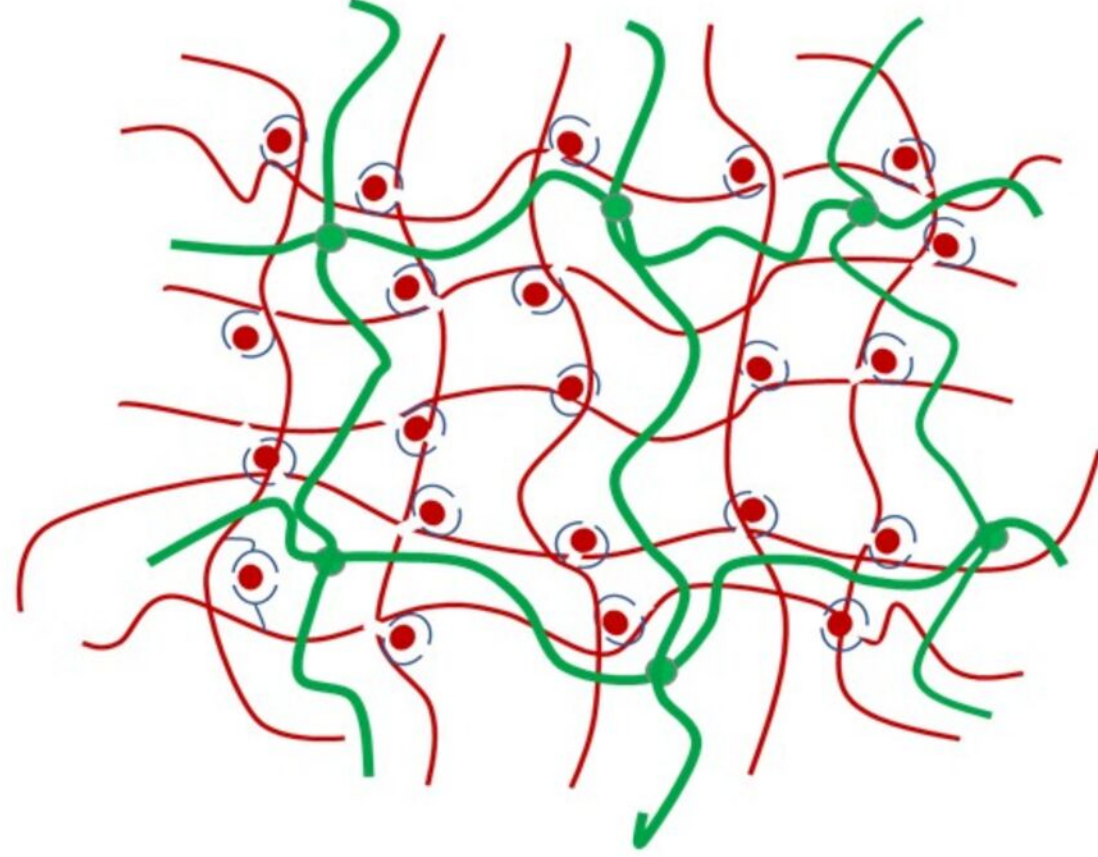


This is the author's peer reviewed, accepted manuscript. However, the online version of record will be different from this version once it has been copyedited and typeset.
PLEASE CITE THIS ARTICLE AS DOI: 10.1122/8.0000473



This is the author's peer reviewed, accepted manuscript. However, the online version of record will be different from this version once it has been copyedited and typeset.
PLEASE CITE THIS ARTICLE AS DOI: 10.1122/8.0000473

(a)



(b)

